Gas chromatography

(Article begins on next page)

26 December 2024

CHEMICAL ANALYSIS OF FOOD Second Edition: TECHNIQUES AND APPLICATIONS

9. Gas Chromatography

Chiara Cordero[1]*, Cecilia Cagliero[1], Erica Liberto[1], Barbara Sgorbini[1], Patrizia Rubiolo[1] and Carlo Bicchi[1]

[1] Dipartimento di Scienza e Tecnologia del Farmaco,
Università degli Studi di Torino,
Via Pietro Giuria n°9
10125 Torino, Italy

* Corresponding author

Address for correspondence: Dr. Chiara Cordero,
Dipartimento di Scienza e Tecnologia del Farmaco, Università degli Studi di Torino, Via Pietro Giuria 9, I-10125 Torino, Italy
Phone: +39 011 6707662 - Fax +39 011 2367172
e-mail: chiara.cordero@unito.it

Summary

This chapter provides a survey about state-of-the-art, technology and instrumental solutions for gas chromatography applied to food chemical characterization; cutting-edge applications; future trends are also presented.

The aim is to deal with some of the most recent innovations on: (a) column technology as new generations of stationary phases and miniaturization; (b) multidimensional platforms combining liquid chromatography to gas chromatography for samples pre-fractionation and in-depth characterization; (c) comprehensive two-dimensional gas chromatography as the most recent and straightforward technological aldvancement of GC.

The role of mass spectrometric detection is also discussed in terms of information provided for confident analytes identification and profiling potentials while the high-resolution mass spectrometry and hard- and soft ionization options are reviewed for their relevance in food quality assessment and safety.

9.1 Introduction

Since its introduction in the early 1950s, gas chromatography (GC) has demonstrated to be an effective, flexible and sensitive analytical technique for in-depth chemical characterization of food samples. In particular, it can be considered the technique of choice for food volatiles profiling (aroma and flavor), for the identification and quantitation of organic contaminants and residues in food, for origin authentication and more generally to verify the compliance with quality standards and safety requirements.

This chapter is intended as an update of our previous contribution in the first edition of "Chemical Analysis of Food" and provides a critical review on the most recent advances and technologies that impacted on GC in the last ten-to-fifteen years.

In the first part column technology and innovation on GC stationary phases are discussed, then multidimensional platforms for LC-GC and GC×GC are illustrated for their potentials in complex food analysis. Last but not least, an eye on the role of mass spectrometry is given by discussing the potentials of new soft-ionization technologies and the benefits they add to food applications.

9.2 Advances in column technology

The miniaturization of gas chromatographic systems can be obtained either by scaling down single components (injector, column and detector) or by implementing microfluidic devices realized by microelectromechanical systems (MEMS) technology (Mittermüller & Volmer, 2012).

The first GC on a chip was by silicon micromachining and dates late 1970s; it was developed by Terry et al. (Terry, Herman, & Angell, 1979) and consisted of an injection valve connected to a 1.5 m planar column and a thermal conductivity detector. These components were realized in two wafers. For a more comprehensive review of the state-of-the-art of GC on-a-chip, the paper from Haghighi et al. (Haghighi, Talebpour, & Sanati-Nezhad, 2015) is recommended. The

paper provides a general overview with comprehensive coverage of the topic with a particular focus on materials and fabrication techniques, chip-based injectors and pre-concentrators, planar columns and their geometry, and detectors. Information about approaches to planar column technologies, available stationary phases and application fields are reviewed by Azzouz et al (Azzouz et al., 2014).

Terry et al. (Terry et al., 1979) were the first introducing planar columns, also referred to as microchannels, MEMS columns, or microfabricated columns, by MEMS technology. They are prepared by a gas phase reactive ion etching process, that produces rectangular open channels on a silicon wafer substrate; the wafer is then sealed with either a silicon or a Pyrex glass plate bonded to the silicon surface. Planar column can be subjected to fast heating gradients by thin film resistance heating patterned in etched silicon channels. This solution enables the simplification of the entire miniaturized GC system by eliminating conventional convection oven modules. Resistance heating carries also some additional advantages as energy saving and providing rapid heating rates particularly useful to increase the speed of separation with short columns (Smith, 2012).

On-chip GC is connoted by obvious benefits in terms of saving energy, materials, and laboratory space although compact analytical platforms should offer technical characteristics and performances comparable to conventional systems. Undoubtedly, on-chip systems are fundamental to realize portable GC for "in-field" analyses. Successful applications are those in environmental control, in mineral oil industry, and in forensic to control toxicants and explosives (Azzouz et al., 2014).

A field of interest for at-line and on-line GC monitoring could be that related to plant food volatiles. The volatile fraction of edible plants is generally very complex, it often consists of hundreds of volatiles within a limited range of molecular weights, similar chemical functionalities and structure, with common physicochemical characteristics including polarity and volatility. Their chemical profiling requires highly efficient and selective

analysis systems providing sufficient discrimination and resolution.

Besides the intrinsic complexity of plant volatile fraction, its in-field and laboratory chemical characterization is a field in which on-chip GC offers very interesting perspectives, and to date has been under-investigated (Cagliero et al., 2016).

On-chip GC if implemented with on-line sample preparation and/or micro-concentration systems could be successful to promptly monitor the evolution of volatiles blend in toto or for specific markers; applications of interest cover: (a) plant maturation processes, (b) studies of ecological biochemistry and/or multitrophic phenomena, (c) chemotaxonomy, and (d) at-line control of essential oils or extracts production (Cagliero et al., 2014) (Rubiolo, Sgorbini, Liberto, Cordero, & Bicchi, 2010).

To evaluate the possible application of on-chip GC to profile plant volatiles, Cagliero et al. (Cagliero et al., 2016) recently evaluated the performance of planar columns of different dimensions and coated with different stationary phases, installed in a conventional GC. Performances were compared to those from conventional narrow bore GC columns.

In particular, authors tested planar columns of different geometry, coated with 5%-phenyl-polymethylsiloxane (Sil-5%-PH) and auto-bondable nitroterephthalic-acid-modified polyethylene glycol (FFAP–EXT).

The micromachined circular double–spiral-shaped channel planar columns illustrated in Figure 9.1 were fabricated by silicon direct bonding of the two wafers (1.5 × 1.5 cm^2). One of them had rectangular (or square) channels and was etched using a Deep Reactive Ion Etching (D-RIE) with a silicon oxide mask layer. Total column length and etched channels dimensions are detailed in Table 9.1. Onto the second wafer, holes for inlet and outlet were bored using D-RIE. As final step, after wafer bonding and singulation, deactivated fused silica capillaries (25 cm long, d_c:0.1 mm) were inserted into the inlet/outlet holes by standard fluidic interconnections made on the chip, and sealed with a polyimide resin. As a term of comparison, a nominal channel inner diameter (nd_c) for each planar column to be used was calculated through the

following expression: $nd_c = 2(S/\pi)1/2$ where S is the area of the channel section.

Planar column coating was by the static procedure and is well-detailed in the reference by Cagliero et al. (Cagliero et al., 2016).

The volatile fractions investigated were obtained by essential oil hydrodistillation or headspace sampling. The two methods are based on different principles (hydrodistillation and vaporization) but they both provide representative but not comparable fractions.

The performances of planar and reference columns were assessed by evaluating the Grob test results in terms of inertness, efficiency, and retention. As indicated in Table 9.1, results confirmed column inertness accompanied by a good efficiency; theoretical plate number per meter (N/m) ranged between 6100 and 7200 for conventional SP.

Their application to real samples is illustrated for chamomile (*Matricaria chamomilla* L.) volatile fraction, whose composition mainly consists of sesquitepenoids. Figure 9.2 illustrates the GC patterns (a) of the chamomile e.o., and (b) of the headspace from the same plant material sampled by SPME obtained on a thin-film FFAP–EXT planar column (Column 2 in Table 9.1) and on the reference NB column (Ref 2 in Table 9.1). The chamomile volatiles profile from planar column (solid lines) perfectly overlaps that of the conventional NB column (dashed lines); this is true for both the e.o. and for the HS-SPME sampling.

Another interesting example is that from sage (S. officinalis L.) e.o., in this case authors investigated the reliability of linear retention indices ($I^T{}_S$) (van Den Dool & Dec. Kratz, 1963) achieved with planar columns and compared them to those obtained with the corresponding conventional NB column. $I^T{}_S$ are fundamental for confident identification of analytes in particular for in-field analysis where the combination of micro-GC with mass spectrometry is still at an early stage of development. Sage e.o. is characterized by a series of terpenoids ranging from monoterpene hydrocarbons (C10, e.g. α- and β-pinene) to diterpenic alcohols (C20, e.g. sclareol). In this case sage was analyzed using a Sil −5% -PH planar and a NB column, and $I^T{}_S$ calculated versus a C9–C25 hydrocarbon standard mixture.

Fig. 9.3 shows GC profiles of the sage e.o., obtained with (A) the Sil −5% -PH column 1, and (B) the corresponding NB column, while Table 9.2 lists retention indices and percent chromatographic area of sage components (normalization is on ethyl dodecanoate). Results confirm the reliability of chromatographic performances of planar columns compared to NB reference columns. Comparability is on both: qualitative terms where I^T_S varying by a maximum of 7 units and in quantitative terms where normalized peak areas do not exceed 10% of relative standard deviation (RSD).

Results obtained by Cagliero et al. (Cagliero et al., 2016) show that planar columns can successfully be used for in-field analysis of plant volatiles by a lab-on-chip GC. Column performances are compatible to general principles for a correct analysis and also comparable to those of conventional narrow-bore columns. The possibility to adopt, with great confidence linear retention indexing is very important as well as the consistency of quantitative descriptors (i.e. % chromatographic areas) that help quality assessment and conformity evaluation of samples.

Future developments aimed at realizing injection systems consisting of planar microconcentrators suitable for a direct connection to the planar columns. In a final lab-on-chip GC configuration, planar columns will be packaged at chip level with planar MEMS injectors and detectors and heated on-chip using thin-film metal heating resistors. This would significantly contribute to increase planar column efficiency because of the drastic reduction of the void volumes.

9.3 New generations of stationary phases

Ionic liquids stationary phases

The development and commercial introduction of ionic liquid (IL) stationary phases for capillary columns is undoubtedly one of the most recent advances in gas chromatography. These columns have been applied for chemical characterization of samples in several fields including environmental samples, petroleum derivatives,

biological fluids, foods, natural products and others. IL stationary phases are successful in the separation of medium and high polarity analytes in both conventional and multidimensional GC (Amaral, Marriott, Bizzo, & Rezende, 2018). Particularly noteworthy is the analysis of fatty acid methyl esters (FAME) from food samples (Kulsing et al., 2014).

ILs are organic molten salts with melting point lower than 100 °C. For those salts showing a melting point below room temperature, liquids are named room temperature ionic liquid (RTIL) (Berthod, Ruiz-Ángel, & Carda-Broch, 2018). Their rediscovery is dated at the end of the last century, and up to now they have been considered for several applications including organic syntheses and chemical engineering, where ILs can act as catalysts or solvents, or as starting point to prepare new materials for pharmaceutical and environmental science due to their versatility and "green" character.

ILs consists of large organic cations combined with several different anions. Within the most common cations, it has to be mentioned imidazolium, pyridinium, pyrrolidinium and their related mono or poly-alkyl derivatives, tetraalkyl ammonium or phosphonium and trialkyl sulfonium. On the other hand, common IL anions include: bis(trifluoromethyl sulfonyl)imide (NTf_2), trifluoromethylsulfate (TfO), dicyanamide ($N(CN)_2$), tetrafluoroborate (BF_4) or hexafluorophosphate (PF_6).

ILs have physicochemical properties that make them suitable for GC. Key-characteristics include: melting point, viscosity, vapor pressure, thermal stability and solvent properties.

Melting point, for example, can be tuned by designing salts consisting of large and asymmetrical ions. Alkyl-methylimidazolium-PF_6 ILs have their minimal m.p. value at −61 °C with 1-hexyl-3-methylimidazolium PF_6, with a C6 chain included in the molecular structure. On the other hand, shorter alkyl chains (n < 6) improving ion cohesion result in higher melting points while longer alkyl chains (n > 8) increase cations hydrophobicity thanks to Van der Waals interaction with further increase of the m.p.

Vapor pressure as well as thermal stability of ILs are fundamental features when used as stationary phases in gas chromatography.

Although ILs are considered as non-volatile solvents, they have a low, measurable vapor pressure, e.g.   for NTf$_2$ ILs, vapor pressure decreases as the alkyl chain length increases. The reference literature is recommended to the reader interested to deepen these aspects (Berthod et al., 2018).

ILs thermal stability becomes fundamental when they are adopted as GC stationary phases. Di-cationic imidazolidinium and phosphorous based ILs are stable up to 425 °C. Table 9.2 lists molecular structures and physico-chemical properties of a series of di- and tri-cationic ILs extensively studied for peculiar selectivity compared to existing polar GC stationary phases (Payagala et al., 2009).

Reichardt evaluatedILs polarity for a wide variety of structures finding that it accounted between *ET(30)* of 43.9 for tetrahexylammonium benzoate IL and 60.8 for 2-hydroxyethyl-3-methyl imidazolium bis(trifluoromethylsulfonyl) imide IL (Reichardt, 2005). Common polar considered solvents as acetone, acetonitrile, methanol, and water have *ET(30)* values respectively of 42.3, 45.6, 55.4, and 63.1.

Therefore, most of the ILs fall within a narrow but high *ET(30)* molecular polarity range with an additional ionic character that gives them an original behaviour as solvents.

Commercially available IL-coated capillary GC columns are marketed by Millipore-Sigma under the trade name SLB-IL followed by a number that refers to column polarity. For example, SLB-IL60 column has a Rochschneider McReynolds index of 2760 while the SLB-IL111 index is 4938 (ref. Table 9.2); SLB-IL60 has a rather polar attitude while IL111 has a polarity index never measured before. These columns have also rather original selectivity and stability over 200 °C up to 300 °C.

This unique, orthogonal selectivity, shown by ILs was exploited in comprehensive two-dimensional gas chromatography by combining short IL columns in the second dimension. In 2D-GC analyses of FAMEs, Nolvachai et al. (Nolvachai, Kulsing, & Marriott, 2015) demonstrated the selectivity of SLB-IL111 operated by temperature programming. Very interestingly, the authors coupled a conventional

30-m SLB-IL111 column (250 μm, 0.2 μm film) to a short narrow bore (100 μm i.d.) SLB-IL111 ionic liquid column with a very thin film (0.08 μm). Such a configuration, theoretical exerting zero orthogonality, provided very high chromatographic resolution and highly informative group-type separation.

An interesting example of challenging separation conducted by IL columns is that proposed by Amaral et al. (Amaral et al., 2018) on roasted coffee volatiles. Its volatile fraction is composed more than thousand compounds belonging to several chemical classes or groups; pyrazines and furans are above all predominant in terms of number of analytes detectable and concentration in the sample. The authors compared the chromatographic performance of a selection of commercial ionic liquid stationary phases to that of polyethylene glycol (PEG). Headspace solid-phase microextraction (HS-SPME) was applied to sample volatiles from commercial samples of roasted and ground coffee. Figure 9.4 shows chromatographic profiles of a roasted coffee sample volatiles obtained by a PEG column (i.e., DB-Wax, Agilent Technologies) and three commercial IL columns: SLB-IL60, SLB-IL76 and SLB-IL111. IL columns showed a low bleeding, relatively high thermal stability and and extended temperature range thus enabling to identify uniquely many compounds with a basic character, such as pyrazines. and pyridines.

Despite the lower number of separated compounds, i.e., 136 identifyed on the DB-Wax profiles vs. 96, 64 and 68 from SLB-IL60, SLB-IL76 and SLB-IL111 respectively, suggesting an inertness problem (Amaral et al., 2018), IL columns and in particular SLB-IL60, were very effective to separate key-analytes such as 3,4-dimethyl-2,5-furanedione, 2,3-diethyl-5-methyl-pyrazine and 5-methyl-(5H)-6,7-dihydrocyclopentapyrazine. These heterocycles were not identified in the DB-Wax profile. The authors tentatively identified some additional compounds in their samples less frequently cited in literature: pyrrolo[1,2-a]pyrazine; nicotinic alcohol; methyl nicotinate; catechol; 2-hydroxy-3-propyl-2-cyclopenten-1-one, 6-methyl-3-pyridinol, 1-(3-thienyl)-ethanone, 2-methyl-3-pyridinol and 4-methyl-2(1H)-quinolinone; and 3-methyl-indole. In the analyses of reference compounds used for identity confirmation, the

authors observed strong interactions of SLB-IL76 and IL111 with acids, furanones and vanillin. On the other hand, changes in the elution order enabled better separations for pyrazines 2-ethyl-3-methylpyrazine/2,3,5-trimethylpyrazine, which co-eluted with DB-Wax.

As additional feature of IL columns, several authors observed that retention times are generally lower compared to standard polar columns; this aspect could be of help in routine control analyses, improving productivity and reducing equipment costs (Amaral et al., 2018).

In conclusion, interesting features, such as high polarity, tunable selectivity and relatively low bleeding (thermal stability), characterize IL stationary phases. These factors can favour the selection of these columns for challenging separations in those samples where standard polar stationary phases show some limitations. future targets for manufacturer include improvements in selectivity and inertness.

Water compatible stationary phases

Very recently, Millipore commercially introduced ILs columns dedicated to water analysis under the the trade name i.e., Watercol™. These stationary phases enable direct injection of aqueous samples in GC opening new opportunities for the analysis of water-based samples without the need of dedicated sample preparation procedures to eliminate this interfering medium. ILs adopted to realize Watercol™ are those studied by Armstrong's group (Armstrong, Jayawardhana, Woods, Zhang, & Wang, 2011) and are based on phosphonium- and imidazolium-derived cations, combined with anions consisting of 2 or 3 units of trifluoromethanesulphonate. These columns have very good performances in terms of selectivity and stability over time.

An interesting application, dealing with food quality and safety assessment, has been recently presented by Sgorbini et al. (Sgorbini et al., 2019), who presented a straightforward method to quantify quality markers in herbal teas.

Because of their biological activities, herbal teas are often used in traditional medicine and more in general by consumers for their pleasant aroma and taste. From a safety standpoint, some bioactive compounds may be toxicologically relevant and may exert adverse effects when consumed above a certain amount. Moreover, while commercially-available herbal teabags contain a weighed and standardized amount of herb content, raw plant materials, as such or in a blend, are often prepared using unspecified quantities. At the same time, preparation procedures and number of consumed cups per day may vary the consumer exposure to volatile bioactive compounds.

The analytical and botanical quality controls are therefore mandatory to guarantee their effective and safe use. Quality control should be qualitative to definemarker compounds or quantitative and accurate to inform about the absolute amount of volatiles of concerns. International regulatory organizations (e.g. the European Medicinal Agency (EMA) or the World Health Organization (WHO)), for instance, have established a maximum daily exposure of 6 and 3.5 mg, respectively, for α- and β-thujone, and 10 μg/Kg/day for estragole. The Joint FAO/WHO Expert Committee on Food Additives (JECFA) recommended an accepted daily intake below 2.0 mg/kg/day and below 4.0 mg/kg/dayfor anethole and menthol, respectively.

Sgorbini et al. (Sgorbini et al., 2019) explored the possibility of a direct injection of the aqueous herbal teas into a GC-FID system and, by using water-compatible ionic liquid coated columns, they separated and accurately quantified analytes of concerns. Authors demonstrated that the direct injection (DAI) GC-FID method complies with specifications for routine quality control analyses, achieving an adequate sensitivity while providing reliable, accurate and repeatable results. In addition, a reduction of the total analysis time by a factor of two (from 100 min to 50 min) was also achieved by eliminating intermediate steps related to sample preparation, the use of accumulating materials (SPME fibers) and additional instrumentation (e.g. thermostatic system). Figure 9.5 illustrates the chromatographic profiles of peppermint volatiles from dried plant material (Fig. 9.5 A) used for teabags preparation together with

those obtained by direct immersion SPME (Fig. 9.5 B) and/or direct injection (DAI) of peppermint herbal tea (Fig. 9.5 C). Markers are all detectable (1,8-cineole, γ-terpinene, menthone, isomenthone, menthol, and menthyl acetate) within a suitable linearity range for their accurate quantitation. Quantitative results, obtained by external standard procedure, in the plant material and in the herbal tea enabled to calculate the extraction rate and the amount of regulated compounds in the final cup.

Figure 9.5 C shows the water peak (i.e., *w*) eluting after a hydrophobic interferent; water has a symmetrical shape and is well resolved from its neighbours.

9.4 Multidimensional Gas Chromatographic platforms

LC-GC systems instrumental configurations

The chemical characterization of complex samples has been the driving force behind innovation and improvements on established approaches and techniques. In GC, the introduction of capillary columns, to replace packed columns, have 10 times increased the separation power unraveling unexpected complexity in several "known" samples. The GC coupling to mass spectrometry (low- or high- resolution MS) have added an additional analytical dimension to every run enabling a better understanding of the nature of complex samples and their actual chemical dimensionality (Giddings, 1995).

In this direction, multidimensional chromatography (MDC) based on both heart-cutting (HC/MDC) or comprehensive (GC×GC) principles, have opened new perspectives to investigate more effectively food samples complexity and composition. However, in some cases, let's say very challenging, MDGC techniques are still insufficient. The coupling of two different chromatographic approaches (e.g., LC-GC, LC×GC) has been investigated over the years ans in some cases has offered unique and straightforward solutions.

In this section, the LC-GC coupling is briefly presented as it represents a solution of choice for pre-fractionation and clean-up of

complex food samples when mineral oil hydrocarbons (MOH) contamination has to be assessed.

The first commercial LC-GC platform was introduced in 1989 by Carlo Erba (Thermo Fisher, Austin Texas) and in 1991 the system was coupled to a MS detector for polycyclic aromatic hydrocarbons (PAHs) analysis in vegetable oils (Vreuls, de Jong, & Brinkman, 1991).

LC-GC is a very powerful approach, it enables efficient sample clean-up and, based on the LC separation principles in the first dimension, group-type separation of analytes is also possible. These key-features have a return on method sensitivity and selectivity. Furthermore, operating by "on-line" sequential separations, sample manipulation is minimized, analysis time is shorter and cross-contamination or artifact formation due to atmospheric oxygen or moisture exposure are limited if not eliminated.

Any LC-GC platform is composed by three elements: a LC, a GC an interface capable of transferring fractions from the LC into the GC. The LC has to pre-fractionate the sample reaching the second step while the GC performs the analytical separation before detection that, depending on the application requirements, can be a flame ionization detector (FID), a MS or both operating in parallel (Purcaro, Moret, & Conte, 2013).

The LC dimension of the system is generally equipped with normal-phase (NP) stationary phases; this is because the eluents are suitable for GC. Reversed-phase (RP) chromatography has been proposed although less frequently adopted due to the incompatibility of many solvents with GC phases.

Column dimensions and flow-rates should fit the evaporation rate necessary to transfer eluting fractions into the GC; the 2-mm i.d. columns with LC flows of about 0.3–0.5 mL/min are the most often used.

The heart of any LC-GC system is the transfer interface; over the years, this has been the focus of most instrumental developments and innovation.

The retention-gap interface is technically inspired by the on-column (OC) large volume injection (LVI) approach. The LC eluent goes through a switching valve to the waste and, during the transfer

step, passes through a rather long capillary retention gap (5–10 m) of wide internal diameter (0.53 mm i.d.) connected by a Tee-union to the analytical GC column and to a solvent-vapor exit (SVE). The transfer can be done by partial or full concurrent eluent evaporation (M Biedermann & Grob, 2009). They differ for the transfer temperature adopted that can be below or at the solvent boiling point, respectively. A faster transfer is obtained with the fully concurrent eluent evaporation although it may cause loss of the most volatile analytes. The OC interface evolved, in 2009, into the so called Y interface that reduces memory effects. This Y interface, in its original design, is commercialized by Brechbühler (Switzerland) while, other instruments are available with a modified design. SRA Intruments (Milan, Italy) implemented a flow-cell autoinjector system to transfer the fraction of interest into the OC injector.

Another interface is that inspired by the pioneering experiments of Majors in 1980 (Majors, 1980)that adopted a split/splitless flash-vaporization injector to transfer small sample volumes (0.1–3 µL). This instrumental solution was refined by David and co-workers (David, Hoffmann, & Sandra, 1999) who proposed the use of a PTV injector to enable larger volumes injection. The PTV is, in this case, equipped with a packed liner capable of retaining more liquid sample per volume unit compared to a capillary retention gap. This instrumental solution is available from Shimadzu (Japan).

The most recent transfer interface, in terms of design and operation principles, was introduced in 1999 and was called TOTAD (Through Oven Transfer Adsorption Desorption) (Perez, Alario, Vazquez, & Villén, 1999). Here a PTV injector is installed horizontally on a side of the GC oven with the inlet carrier gas connected alternately to the normal inlet and the split-exit port. Both LC and the GC transfer lines are connected at the bottom of the PTV injector. During the transfer step, the LC eluent goes through a Tenax™-packed liner and the carrier gas entering through the split-exit port facilitates solvent evaporation. Solvent vapors exit is by a stainless-steel tube installed through the inlet septum. After evaporation, the PTV injector is heated, carrier gas inlet switched to the usual one while solutes enter into the GC column. This interface is

commercialized by Konik-Tech (Spain).

About the GC dimension, particular attention has to be paid for the retention-gap technique where a pre-column is needed. The pre-column should have certain features as wettability by the solvent to form a liquid film on the internal wall, inertness and a minimal retention power that guarantees band reconcentration before GC separation. Retention gap internal diameter has to be large enough to allow high vapor-flow rate exit for an efficient discharge of the LC eluent.

LC-GC application to mineral oil contamination assessment

Mineral oil (MO) contamination in food is one of the main fiel of application where LC-GC exploits its characteristic features. MO are formed by a wide range of highly lipophilic compounds deriving from petroleum distillation; they primarily contain saturated hydrocarbons, referred to as MO saturated hydrocarbons (MOSH), and, to some extent, MO aromatic hydrocarbons (MOAH), mainly alkylated PAHs. MO compounds are used as ingredients in cosmetic products or as additives their presence in food is generally considered as nonintended contaminantion. They have wide application in technical products including food contact materials such as packagings therefore their migration into foods, most easily into fat-containing food, is frequent. Analytical methodologies suitable for pure mineral oil products characterization do not show sufficient sensitivity to detect trace amount contamination of MO into foods. Therefore, the development of new methods implementing the LC-GC approach conducted to the first successful solution presented by Grob in 1991 (Grob, Lanfranchi, Egli, & Artho, 1991).

Normal phase LC columns, such as silica-gel, can retain fat and other food constituents that may interfere with MO characterization and quantitation. The first application focusing on the determination of the MOAH fraction in food was presented in 1996 by Moret et al. (Moret, Grob, & Conte, 1996); authors developed a LC-LC-GC system where a first silica column (25 cm × 4.6 m i.d.) was used to elute the

entire MOAH fraction in a 6–8 mL. The solvent was not compatible with the second LC dimension consisting of an aminosilane stationary phase (10 cm × 4.6 mm i.d.) therefore, a miniaturized solvent evaporator (SE) was on-line inserted between the two columns. In this second dimension, paraffins were separated from MOAH, which were also fractionated according to the number of rings. An additional back-flush valve was connected to the second column, it switched immediately after paraffin elution, enabled to quantify aromatics in a single fraction.

Nowadays, a standardized procedure based on LC-GC-FID MD platform, is available to detect MOSH/MOAH concentrations of about 10 mg/kg in food matrices. The European norm (EN) 16995 includes a sample preparation step based on solvent extraction by CH_2Cl_2/hexane 3:7 (v/v) for fats and oils or by ethanol and hexane for fatty food containing water. Extraction is followed by a clean-up step, when necessary, by solid phase extraction (SPE) on aluminium oxide for the MOSH fraction and by epoxidation for the MOAH fraction. Extracts are then submitted to LC-GC-FID on a NP Silica column (250 mm x 2 mm id x 5 um) with hexane/ CH_2Cl_2 as eluent. The GC step is by a short apolar GC column with a thinner film (OV1 or SE 52 15 m x 0.32-0.25 mm id x 0.10 um) directly connected to a FID detector. If interfering compounds are expected, the EN norm recommends the confirmation of the fossil origin of MOSH/MOAH by GCxGC-MS. To establish the MO contamination, the peak area corresponding to mineral oil elution "hump" is determined after subtraction of n-alkanes peaks, terpenes, squalene and its isomerization products, styrenes, and olefins with carotenoid structure. MOSH and MOAH are then quantified using a suitable internal standard, added before the analysis, and by applying FID response factors. Several internal standards are also included to monitor LC fractionation consistency and GC transfer reliability. Figure 9.6 shows the MOSH and MOAH chromatograms obtained by a food contact material made by fresh fibres and printed with a mineral oil containing ink (left) and a fresh fiber paper tea bag contaminated by a mineral ink oil and an oil used for paper making. Profiles were obtained according to the procedure illustrated by

Biedermann and Grob (M Biedermann & Grob, 2012).

Mineral oils that contaminates food consist almost exclusively of branched compounds; these analytes are not retained on activated aluminum oxide therefore it is the ideal sorbent to remove plant-based paraffins that may interfere with MOSH quantitation. On the other hand, the elution behaviour of MOSH and MOAH is sometimes not sufficiently specific therefore, MOAH fraction may results contaminated by a carry-over or a strong interference by non-aromatic hydrocarbons. Scientific literature reports initial evidence that LC-GC-FID may possibly overestimate MOAH compared with more specific methods such as NMR (Weber et al., 2018).

More generally, confirmatory methods, including mass selective detector and/or comprehensive 2D-GC separation are needed to achieve detailed identification of MOSH and MOAH fractions while confirming the consistency of qurntitative results.

Straighforward solutions are nowadays available in this field, LC-GC×GC-FID/MS combining orthogonal separation principles and detection concepts represent the future for this field. Readers interested to go more in depth in this topic could refer to the following literature (Biedermann, Munoz, & Grob, 2017; Gharbi et al., 2017; Grob, 2018a, 2018b).

The outstanding results obtained with multi-dimensional systems clearly demonstrate that behind any "apparently" simple matrix a much more complex chemical profile could be hidden. However, it is also clear that, a third dimension at the separation or at the detection level by MS, is often useful to solve ambiguities and provide more accurate results.

9.5 Comprehensive Two-dimensional Gas Chromatography

One of the most straightforward advances in the field of gas chromatography achieved in the last 15 years is undoubtedly comprehensive two-dimensional GC. This MDC technique can be today considered mature, also thanks to the presence of several commercial solutions on the market, and also well established and recognized in some fields where is the technique of choice, e.g.

petroleomics applications. Its adoption in food chemical characterization is growing and several research groups, working in this field, have shaded light on its potentials and on the advantages provided by its separation power and sensitivity.

The reasons at the basis of the adoption of any MDGC approach are delineated by the Giddings's definition: MDGC "*provides a means for greatly enhancing the peak capacity and thus the resolution of the components of complex mixtures....*"(Giddings, 1995). Within the context of MDGC, comprehensive separations by GC×GC, when performed in optimized conditions, can achieve a peak capacity per unit run-time approximately of an order of magnitude greater than conventional 1D-GC.

This section will illustrate some of the most recent and straightforward research in the field of GC×GC, devoted to food applications, where system resolution, separation power and information potential have been exploited by introducing innovative analytical set-up or by dedicated data processing strategies.

Improving GC×GC separation power and resolution

In this perspective, the design of the chromatographic set-up by combining columns with different diameters and stationary phases in the two chromatographic dimensions is fundamental at the method development stage. Most GC×GC set-up consist of a long, conventional-inner-diameter first-dimension (^{1}D) column (15-30 m and 0.32-0.25 mm d_c), and a short, narrow-bore second-dimension (^{2}D) column (0.5–2 m and 0.1 mm d_c). The ^{2}D separation is thereby completed in a few seconds, corresponding to the modulation period (P_M), and system efficiency is maximized.

However, in those systems equipped with thermal modulator, also referred to as cryogenic modulators (Tranchida, Purcaro, Dugo, Mondello, 2011), the two GC columns are coupled in series generating a flow mismatch between the two dimensions. This thereby affects the separation efficiency since it is impossible to operate at optimized flow conditions in both dimensions (Beens, Janssen, Adahchour, & Brinkman, 2005). As an aid to method

development, Beens et al. (Beens, Blomberg, & Schoenmakers, 2000) developed a computer program, based on Excel®, that assists analysts in selecting appropriate column set-up and carrier gas flows.

To extend GC×GC separation capabilities while providing also more flexibility in terms of selectivity and resolution, Sharif et al. (K.M. Sharif, Kulsing, Junior, & Marriott, 2017; Khan M. Sharif, Kulsing, & Marriott, 2016) exploited the concept of pressure tuning (PT) operated either on the ^{1}D or on the ^{2}D. They connected two ^{1}D columns (^{1}D1 and ^{1}D2) in series via a microfluidic splitter device; then a conventional ^{2}D narrow bore column was used to complete the system set-up. By varying the pressure between the ^{1}D1 and ^{1}D2 columns, carrier gas is subjected to decompression and results in a tunable pressure-drop across each ^{1}D. This condition affects analytes retention in both absolute and relative terms. Interestingly, PT influences also the ^{2}D retention because of the elution temperature differences. PT has a direct impact on the selectivity of the entire system while making its orthogonality "tunable". Odorants and quality markers of Australian tea tree oil (i.e., monoterpenes, sesquiterpenes, and oxygenated terpenes) were investigated by PT-GC×GC. Figure 9.7 shows the 2D patterns of a tea tree oil sample analyzed by varying the pressure at the junction between the two ^{1}D columns (Pj) from 30 to 60 psi and adopting two column set-up exerting different selectivity. The ^{1}D column set consist on a SLB-IL60/SLB-5ms (Fig. 9.7A and 9.7B) or on the reversed combination SLB-5ms/ SLB-IL60 (Fig. 9.7C and 9.7D). The elution order and the overall orthogonality (O) calculated by information theory as O% were drastically affected.

An alternative way to improve system separation power and selectivity by impacting on carrier velocities was proposed by Liu and Phillips (Liu & Phillips, 1994). They designed a Tee union to connect the two analytical dimensions and, by a short capillary, diverted a certain % of the ^{1}D effluent to a waste-line. This operation brought the ^{1}D and ^{2}D carrier flows closer to their optimal values while limiting the overloading of the ^{2}D capillary. This instrumental solution was exploited by Tranchida et al. (Peter Quinto Tranchida, Casilli, Dugo, Dugo, & Mondello, 2007) for Fatty Acids Methyl Esters

(FAMEs) profiling in cod liver oil samples. Figure 9.8 illustrates the 2D-pattern of cod liver oil FAMEs obtained by reducing the ^{2}D carrier gas velocity from 577.2 cm/s to 264 cm/s by applying a flow-splitting of about 20:80. The enlarged area of the 2D chromatogram illustrates the satisfactory resolution obtained for the C16 and C22 clusters with a very good occupation of the chromatographic space that is informative of system orthogonality.

In the field of complex aroma characterization, GC×GC efficiency and resolution are not alone sufficient and have to be accompanied by adequate ^{2}D loadability. This feature avoids, or at least limits, extra-chromatographic effects that may reduce the available separation space. Nicolotti et al. (Nicolotti et al., 2014) proposed a system configuration where two parallel-secondary columns were used instead of a single one in a GC×GC with thermal modulation. The set-up enabled to achieve close-to-optimal gas linear velocities in both chromatographic dimensions while doubling the 2D loadability and detection capability. Two complementary detectors were in fact adopted, a fast quadrupole MS and a FID.

Consistent analyte patterns were obtained from the two detectors and when profiling *Artemisia umbelliformis* Lam. essential oil components resulted well resolved also in critical chromatographic areas where major components overloaded the ^{2}D. In addition, the parallel detection enabled cross-validation of quantitative results (quantitation was based on external standard procedure and was done on MS and FID independently) and extended method linearity range up to four orders of magnitude (Belhassen et al., 2018; Nicolotti et al., 2014; Sgorbini et al., 2015). Positive effects on resolution between critical pairs of odorants are illustrated in Figure 9.9 where the performances of a conventional GC×GC configuration are compared to those from the dual-parallel secondary columns set-up. Analytes with critical separation are nonanal, 2-methylbutyl isovalerate and α-tujone.

Improving GC×GC identification reliability by structured

pattern separations

GC×GC, when the two chromatographic dimensions are coupled to generate suitable orthogonality, has the capability of generating structured 2D-patterns for analytes sharing common chemical functionalities. The combination of stationary phase chemistries accompanied by suitable temperature programming and flow settings (see section *Improving GC×GC separation power and resolution*) results in great advantages for detailed analysis of group/classes of chemicals and homologues. The rational ordering of analytes over the chromatographic space is beneficial to improve identification reliability expecially for unknowns with characteristic but not unique MS signatures (Yan et al., 2017).

There are several examples in literature where group-type separation represents an additional benefit to exploit at the identification level. Food samples are connoted by a high chemical dimensionality (Giddings, 1995) therefore, although well organized over the 2D-space, chemical patterns are frequently overlapped and their response signals not easily extractable by the so called group-tipe pattern analysis (Reichenbach, Tian, Cordero, & Tao, 2012).

Relevant research studies that dealt with informative groups of chemicals in complex food fractions are those from Ryan et al. (Ryan et al., 2004), who adopted a polar × non-polar column combination to delineate rational patterns for alkyl pyrazines in Arabica and Robusta roasted coffee samples. Authors achieved univocal identification by combining I^T_S in the ^{1}D and MS signatures by EI-TOF MS. Group-type separations were also exploited by Cordero et al. (Cordero, Bicchi, & Rubiolo, 2008) for roasted coffee and hazelnuts. They extended the investigation to all detectable volatiles, including key-odorants and Maillard reaction poducts. Chemical classes producing rational patterns were: short chain fatty acids, aliphatic alcohols, linear saturated and unsaturated aldehydes, alkyl pyrazines, furans, and pyrroles.

When structured patterns result overlapped or not easily recognizable, scripting tools that filter and extract relevant information from the MS dimension are of help. Scripting functions

can be designed to isolate and visualize analytes having specific spectral signatures. This operation is widely adopted in group-type characterization in the petrochemical field (Jennerwein, Eschner, Gröger, Wilharm, & Zimmermann, 2014). In food applications, scripting was adopted by Cordero et al. (Cordero et al., 2013) to map homologues series of lactones, saturated aldehydes and methyl-ketones from dried milk samples and by Magagna et al. (Magagna et al., 2017) to isolate alkanes and carbonyl derivatives (saturated and unsaturated linear aldehydes) patterns from black tea volatile fraction. Figure 9.10 shows 2D patterns from commercial black tea samples; volatiles sampled by HS-SPME are separated on a apolar × semi-polar column combination. Figure 9.10B and 9.10C show the resulting 2D images after scripting normal and iso-alkanes and saturated and unsaturated aldehydes. Scripting functions, as well as the analytical conditions, are reported in the figure caption.

Benefits and flexibility of thermal modulation

Thermal modulators (TM), expecially those based on cryogenic focusing (Peter Quinto Tranchida et al., 2011), are very effective for volatiles and odorants profiling since they enable correct separation of highly volatile (C2-C4) compounds that require a very efficient band-focusing in space to avoid break-through and chromatographic distortion. In optimized conditions, the cryogenic focusing by a two-stage jet trapping and release with liquid nitrogen (LN$_2$) as cryogenics, achieves a peak capacity gain (G_n) close to the theoretical one (Klee, Cochran, Merrick, & Blumberg, 2015). This means that GC×GC separation power and resolution can be maximized by carefully tuning the chromatographic conditions without any efficiency loss introduced by the modulator.

In addition, the presence of a thermal modulator/device within a GC×GC platform can extend its flexibility; it was used as cryotrapping device (CT) accessory in many "multi-multidimensional" approaches explored by Marriott and co-workers (Maikhunthod, Morrison, Small, & Marriott, 2010). These authors adopted CT, by longitudinally modulated cryogenic system (LMCS), to trap analytes

and enable switching between GC×GC and targeted multidimensional gas chromatography (i.e., switchable GC×GC/targeted MDGC). The system configuration is illustrated in Figure 9.11. Separate and independent analyses by 1D-GC, GC×GC, and targeted MDGC are possible thanks to a Deans switch microfluidics module and the CT device; the [1]D column effluent can be directed to either one of two [2]D columns in a classical heart-cutting (H/C) operation. CT enables efficient band focusing and reduces band-broadening in space. Solutes can therefore be effectively injected in the respective [2]D.

The system was evaluated in terms of separation potential, flexibility, identification reliability and accurate quantitation of target analytes on a mixture of potent odorants (γ-terpinene, octanol, menthone, iso-menthone, geraniol, geranyl acetate, and bornyl acetate) and on essential oils.

Besides their advantages and flexibility, their relatively wide loading capacity, variable cryo-focusing temperatures and dynamics etc... thermal modulators have also some drawbacks mainly related to hardware and operational costs. Their application to food chemical characterization, although following a constant increasing trend over the years, relates mainly to research studies. Their adoption for routine quality controls and/or high throughput screenings is rather limited (Cordero, Kiefl, Reichenbach;, & Bicchi, 2018). In this perspective, the alternative represented by differential-flow modulations (Bueno & Seeley, 2004) or by temperature independent modulators (Prebihalo et al., 2018) are of great interest and deserve a dedicated section to illustrate their potentials for food applications.

Potentials of differential-flow modulation for high-throughput profiling and fingerprinting

Differential-flow modulators (FMs), based on the original device described by Seeley et al. (Bueno & Seeley, 2004), later modified to achieve better flexibility by Tranchida et al. (Peter Q Tranchida, Franchina, Dugo, & Mondello, 2012) are interesting alternatives to TM. FMs with a simple and effective design, have low operational and hardware costs and very high robustness. Commercial FM devices are nowadays available from Agilent Technologies [R.L. Firor, Application Brief 5989-6078EN, Agilent Technologies, 2007] and SepSolve (INSIGHT modulator http://www.sepsolve.com/separation/). Very recently, LECO LCC has introduced a new design for FM-GC×GC inspired by the recent work of Seeley et al. (Seeley, Schimmel, & Seeley, 2018) for multi-mode modulation. Systems from Agilent and SepSolve implement the concept of reverse-fill/flush injection dynamics (Cordero et al., 2015; Griffith, Winniford, Sun, Edam, & Luong, 2012) that improves band re-injection efficiency, 2D peak-widths and symmetry, while effectively handle the drawback of collection-channel overloading. Figure 9.12 illustrates the reverse-fill/flush differential-flow modulator functioning. Analytes separated by the ^{1}D column enter at the center port of the modulator plate (Column 1 in) and fill the fixed size collection channel, which is connected to a bleeding capillary port (bottom port). The length and diameter of the bleeding capillary are chosen according to the pressure/flow conditions of the columns to provide a minimal flow increase of about 10% to the output of the first column (Giardina et al., 2018). After loading the collection channel, the three-way solenoid micro-valve switch and the EPC module directs flow to the bottom post, then the channel is flushed, typically for 0.10-0.20 seconds, in the reverse direction of the fill-flow into the ^{2}D column at a suitable volumetric flow. The band enters into the ^{2}D columns and undergoes separation in a few seconds. The modulation cycle is then repeated.
FMs have been successful in profiling studies targeting potent odorants in essential oils and flavors (Cordero et al., 2015; Krupčík,

Gorovenko, Špánik, Sandra, & Giardina, 2016), in fragrances and cosmetics (Cordero et al., 2017), and in food samples (Bernal, Manzano, Diego, Bernal, & Nozal, 2014; Manzano et al., 2011a, 2011b). More recently, Magagna et al. (Magagna et al., 2018) discussed the transfer of a fingerprinting method, capable of classifying various cocoa samples of different geographical origins and at different processing stages, from TM GC×GC-MS to FM GC×GC-MS.

The effective transfer was achieved by applying the principles of method translation (Klee & Blumberg, 2002) for fast gas chromatography. The translated method preserved analyte elution order and original method resolution while all metadata related to separated analytes (known and unknowns) were fully transferred by pattern recognition. This last step was achieved by adopting dedicated algorithms based on the template matching algorithm (Reichenbach, Carr, Stoll, & Tao, 2009).

Figure 9.13 shows 2D peak patterns obtained from a reference method developed on a TM-GC×GC platform (Fig. 9.13A) and those from translated methods on a FM platform (Fig. 9.13C-D). Translated conditions enabled the method to preserve its information potential, although with a loss of sensitivity due to the adoption of 0.10 mm d_c columns in the ^{1}D that limited sample loading. Besides this drawback, the transfer of all metadata (identified compounds and reference EI-MS fragmentation patterns) by template matching was consistent and effectively aligned response for most of the detected compounds. The method fingerprinting accuracy, as correct sub-classification of samples, was validated and 13 over 14 key-aroma compounds were successfully detected by FM GC×2GC-MS/FID. In particular: 3-methylbutanal, 2-heptanol, acetic acid, 3-methylbutanoic acid, butanoic acid, 2-methylpropanoic acid, 3,5-diethyl-2-methyl-pyrazine, 2-ethyl-3,5-dimethylpyrazine, 2,3,5-trimethylpyrazine, ethyl-2-methyl butanoate, phenylethyl alcohol, 2-phenylethyl acetate, phenyl acetaldehyde, and dimethyl trisulfide were all mapped keeping method information potential on cocoa aroma quality.

9.6 Mass spectrometry and its fundamental role for confident

characterization of complex samples

Mass spectrometry can be considered an additional analytical dimension in any chromatographic platform. It expands the information potential of chromatography by adding an orthogonal principle for compounds characterization.

Complex samples, or fractions, even when subjected to MDGC analysis may present several co-eluting compounds at the outled of the ^{1}D column. However, in MDGC there is the chance to discriminate co-eluting analytes by the ^{2}D because of the specific interactions with the stationary phase established (dipole-dipole, H-bonding, π-π, etc.). If, even after two separation steps, compounds still co-elute, a further dimension is needed for analyte discrimination. This additional dimension can be mass spectrometry which may discriminate analytes because of specific and/or distinctive fragmentation patterns.

MS is the ideal detector in food investigations, even when not mandatory as in the case of food safety assessment and controls. It provides information suitable for univocal analyte identity confirmation or identification (in the case of high-resolution – HR MS), it has a wide dynamic range and response linearity, high robustness and reliability, while providing the suitable selectivity for targeted investigations where marker analytes are hidden by major components or interferent peaks.

MS, with fast acquisition by time of flight MS (TOF MS) or scanning quadrupole (qMS) analyzers, is the multivariate detector of choice (Prebihalo et al., 2017) for GC and MDGC. Multi-stage MS, as tandem MS or MS/MS, implemented by triple-quandrupoles (QqQ) for low-resolution MS/MS or modern hybrid solutions that combine quadrupole and TOF MS (q-TOF) or q-Orbitrap™ technology for high resolution-MS/MS, are ever more popular and take the scene in food safety assessment. HRMS supports confident analyte identification when exact masses, specific fragments, or mass defects can be extracted from dense chromatographic regions.

On the other hand, MS at nominal mass resolution provides information about analyte identity when combined with Electron

Impact (EI) ionization thanks to the availability of general or dedicated commercial databases (Adams, 1995; "NIST/EPA/NIH Mass Spectral Library with Search Program Data Version: NIST v17," n.d.) or public repositories that collect spectral data and I^T_S on different stationary phases.

In food characterization studies, GC×GC-HR-TOF MS (GC×GC-accTOFMS) was applied by Wong et al. (Wong, Perlmutter, & Marriott, 2017) to profile secondary metabolites in aromatic plants. In *Eucalyptus* spp. leaf oil, for example, the untargeted profiling by GC×GC-HR-TOFMS highlighted about 400 secondary metabolites; 183 of them were tentatively identified, accounting for between 50.8–90.0% of the total ion response and covering various chemical families. The identification strategy adopted, discussed more in detail by the same research group in a later publication focusing on new hop (*Humulus lupulus* L.) genotypes (Yan et al., 2017), included a multi-step procedure with (a) library search and MS spectral similarity evaluation; (b) for candidates similarity match factors above 700, molecular ion and base peaks mass accuracy were verified (± 15 ppm for the base ion); (c) for isobaric compounds, the I^T_S was verified with accettability criterion of ± 20 units; and (d) structured separation patterns over the 2D space interpreted to narrow the selection of the final candidate(s).

In HR-MS systems, soft ionization techniques are made available by manufactures and optioned by analysts. Soft ionization has the potential to help solving identification ambiguities in complex situations where EI produces similar fragmentation patterns, as in the case of structural isomers. Generally, soft ionization preserves information about the molecular ion and minimizes associated structural fragmentation. Available soft-ionization techniques, i.e., chemical ionization (CI), field ionization (FI), and photoionization (PI), often require dedicated ion sources or instrumentation to switch from standard EI to CI acquisition.

Very recently a new patented ion source has been introduced on the market; it features Select-eV™ ionization technology and is capable of Tandem Ionization™ (TI) within a single run [*US patent* number 9,786,480] by multiplexing between two ionization

energies**. The TI acquisition is user-defined within a range of 10-70 eV at a maximum scan rate of 50 Hz per ionization channel. TI provides complementary chemical selectivity and is of interest to distinguish and identify isometric species (Dubois et al., 2017; Peacock, Zhang, & Trimpin, 2017). In addition, low ionization energies are of help to extend the dynamic range in quantitative applications. The absolute amount of ions generated with SI is lower, thereby detector saturation is limited.

In a recent study by our research group (Baroux et al., 2018) the complex volatilome of high-quality cocoa samples was explored by GC×GC-TOF MS and Tandem Ionization™. Within 193 targeted analytes, informative chemicals known for their role in the description of cocoa aroma (key-aroma compounds and potent odorants), post-harvest practices, and technological impacts were present. Within sensory active compounds concurring in the definition of cocoa aroma blueprint (Frauendorfer, Schieberle, & Chieberle, 2008), twenty were identified: 2-methyl-butanal, ethyl 2-methylbutanoate, 2-heptanol, dimethyl trisulfide, 2,3,5-trimethylpyrazine, acetic acid, 2-ethyl-3,6-dimethyl-pyrazine, 2-ethyl-3,5-dimethyl-pyrazine, 2,3-diethyl-5-methylpyrazine, linalool, 2-methyl propanoic acid, ethyl 2-methylpropanoate, butanoic acid, phenyl acetaldehyde, 3-methyl butanoic acid, 1-phenyl ethanol, 2-phenyl ethyl acetate, phenylethyl alcohol, δ-2-decenolactone, and 4-hydroxy-2,5-dimethyl-3(2h)-furanone. Their quali-quantitative distribution informs about cocoa flavor and concur to define the characteristic sensorial notes: earthy, roasty, rancid, sour, sweaty, malty, cocoa, buttery, flowery, honey-like, fruity, green, fatty, sulfury, and phenolic.

In the study, the spectral quality at 70 eV from the multiplexing system was satisfactory, providing proofs on adequate method reliability at the detection level. On the other hand, spectral similarity/dissimilarity between the different ionization energies adopted (70, 12 and 14 eV) was evaluated.

Table 9.3 lists direct match factor (DMF) and reverse match factors (RMF) values for some targeted cocoa analytes for spectral comparisons between: a) 70 eV vs. database (Wiley 7n or NIST 2014);

b) 12 eV vs. 14 eV; c) 12 eV vs. 70 eV; d) 14 eV vs. 70 eV.

Results indicate that spectral dissimilarity between 12 eV and 70 eV is higher compared to that between 14 and 70 eV. Within analytes that show the most dissimilar patterns (lower DMF values), nonanal and limonene are illustrated in Figure 9.14. For nonanal (Fig. 9.14A), lower ionization energies revealed the molecular ion (i.e, 142 m/z) that was not present at 70 eV. Additionally, on the spectrum at 12 eV, the base peak was 98 m/z while at 14 eV and 70 eV, the most abundant fragment was 57 m/z. For limonene (Fig. 9.14B), a terpenoid derivative, lower ionization energies produced higher relative abundances for fragments with higher m/z ratios (i.e., 93, 107 and 121 m/z) and the molecular ion (i.e., 136 m/z) is enhanced.

Lower ionization energies produce fewer fragments resulting in lower spectral/signal intensities. However, for analytes with greatly or at least meaningful reduced fragmentation at lower eV, the signals are enhanced as shown by signal-to-noise ratio SNR values.

Table 9.3 reports SNR values for selected targets at 70 and 12 eV. Streker aldehydes (2-, and 3- methylbutanal), furan derivatives (furfural and 2-furan methanol), and benzaldehyde have higher relative intensities at 12 eV. This interesting pattern evidences the complementary nature of tandem ionization signals and, in this case as quantitative indicator, suggests that lower ionization energies may be beneficial for fingerprinting sensitivity extending the dynamic range of detection. For analytes where 70 eV produces higher SNRs, detector saturation may therefore be a limiting factor and, in these cases, the tandem signal at lower eV may compensate for this.

References

Adams, R. P. (1995). *Identification of Essential Oil Components by Gas Chromatography—Mass Spectroscopy*. New York: Allured Publishing.

Amaral, M. S. S., Marriott, P. J., Bizzo, H. R., & Rezende, C. M. (2018). Ionic liquid capillary columns for analysis of multi-component volatiles by gas chromatography-mass spectrometry: performance, selectivity, activity and retention indices. *Analytical and Bioanalytical Chemistry*, *410*(19), 4615–4632. https://doi.org/10.1007/s00216-017-0718-7

Armstrong, D. W., Jayawardhana, D. A., Woods, R. M., Zhang, Y., & Wang, C. (2011). Rapid, efficient quantification of water in solvents and solvents in water using an ionic liquid-based GC column. *LC-GC Europe*.

Azzouz, I., Vial, J., Thiébaut, D., Haudebourg, R., Danaie, K., Sassiat, P., & Breviere, J. (2014). Review of stationary phases for microelectromechanical systems in gas chromatography: Feasibility and separations. *Analytical and Bioanalytical Chemistry*, *406*(4), 981–994. https://doi.org/10.1007/s00216-013-7168-7

Baroux, L., Alessandro, C., Carlo, B., Sabine, L., Emilie, B., Philippe, M., & Chiara, C. (2018). HIGH QUALITY COCOA FINGERPRINTING - PART II CHALLENGING ODOR ZONES IN COCOA NIBS: THE KEY-ROLE OF MULTIDIMENSIONAL GAS CHROMATOGRAPHY COUPLED WITH MASS SPECTROMETRY AND OLFACTOMETRY. In L. Mondello (Ed.), *Proceedings of the 42nd International Symposium on Capillary Chromatography and 15th GCxGC Symposium* (p. 1). Chromaleont, Messina (Italy).

Beens, J., Blomberg, J., & Schoenmakers, P. J. (2000). Proper Tuning of Comprehensive Two-Dimensional Gas Chromatography (GC×GC) to Optimize the Separation of Complex Oil Fractions. *Journal of High Resolution Chromatography*, *23*(3), 182–188. https://doi.org/10.1002/(SICI)1521-4168(20000301)23:3<182::AID-JHRC182>3.0.CO;2-E

Beens, J., Janssen, H. G., Adahchour, M., & Brinkman, U. A. T. (2005).

Flow regime at ambient outlet pressure and its influence in comprehensive two-dimensional gas chromatography. *Journal of Chromatography A*, *1086*(1–2), 141–150. https://doi.org/10.1016/j.chroma.2005.05.086

Belhassen, E., Bressanello, D., Merle, P., Raynaud, E., Bicchi, C., Chaintreau, A., & Cordero, C. (2018). Routine quantification of 54 allergens in fragrances using comprehensive two-dimensional gas chromatography-quadrupole mass spectrometry with dual parallel secondary columns. Part I: Method development. *Flavour and Fragrance Journal*, *33*(1), 63–74. https://doi.org/10.1002/ffj.3416

Bernal, J., Manzano, P., Diego, J. C., Bernal, J. L., & Nozal, M. J. (2014). Comprehensive two-dimensional gas chromatography coupled with static headspace sampling to analyze volatile compounds: Application to almonds. *Journal of Separation Science*, *37*(6), 675–683. https://doi.org/10.1002/jssc.201301278

Berthod, A., Ruiz-Ángel, M. J., & Carda-Broch, S. (2018). Recent advances on ionic liquid uses in separation techniques. *Journal of Chromatography A*, *1559*, 2–16. https://doi.org/10.1016/j.chroma.2017.09.044

Biedermann, M., & Grob, K. (2009). Memory effects with the on-column interface for on-line coupled high performance liquid chromatography-gas chromatography: The Y-interface. *Journal of Chromatography A*, *1216*(49), 8652–8658. https://doi.org/10.1016/j.chroma.2009.10.039

Biedermann, M., & Grob, K. (2012). On-line coupled high performance liquid chromatography-gas chromatography for the analysis of contamination by mineral oil. Part 1: Method of analysis. *Journal of Chromatography A*, *1255*, 56–75. https://doi.org/10.1016/j.chroma.2012.05.095

Biedermann, M., Ingenhoff, J.-E., Dima, G., Zurfluh, M., Biedermann-Brem, S., Richter, L., … Grob, K. (2013). Migration of mineral oil from printed paperboard into dry foods: Survey of the German market. Part II: Advancement of migration during storage. *European Food Research and Technology, 236*(3), 459–472. https://doi.org/10.1007/s00217-012-1909-2

Biedermann, M., Munoz, C., & Grob, K. (2017). Update of on-line coupled liquid chromatography – gas chromatography for the analysis of mineral oil hydrocarbons in foods and cosmetics. *Journal of Chromatography A*, *1521*, 140–149. https://doi.org/10.1016/j.chroma.2017.09.028

Bueno, P. A., & Seeley, J. V. (2004). Flow-switching device for comprehensive two-dimensional gas chromatography. In *Journal of Chromatography A* (Vol. 1027, pp. 3–10). https://doi.org/10.1016/j.chroma.2003.10.033

Cagliero, C., Galli, S., Galli, M., Elmi, I., Belluce, M., Zampolli, S., … Bicchi, C. (2016). Conventional and enantioselective gas chromatography with microfabricated planar columns for analysis of real-world samples of plant volatile fraction. *Journal of Chromatography A*, *1429*, 329–339. https://doi.org/10.1016/j.chroma.2015.12.037

Cagliero, C., Sgorbini, B., Cordero, C., Liberto, E., Bicchi, C., & Rubiolo, P. (2014). Analytical strategies for multipurpose studies of a plant volatile fraction. *Handbook of Chemical and Biological Plant Analytical Methods*, 1–20.

Cordero, C., Bicchi, C., & Rubiolo, P. (2008). Group-type and fingerprint analysis of roasted food matrices (coffee and hazelnut samples) by comprehensive two-dimensional gas chromatography. *Journal of Agricultural and Food Chemistry*, *56*(17), 7655–7666. https://doi.org/10.1021/jf801001z

Cordero, C., Cagliero, C., Liberto, E., Nicolotti, L., Rubiolo, P., Sgorbini, B., & Bicchi, C. (2013). High concentration capacity sample preparation techniques to improve the informative potential of two-dimensional comprehensive gas chromatography-mass spectrometry: Application to sensomics. *Journal of Chromatography A*, *1318*, 1–11. https://doi.org/10.1016/j.chroma.2013.09.065

Cordero, C., Kiefl, J., Reichenbach;, S. E., & Bicchi, C. (2018). Characterization of odorant patterns by comprehensive two-dimensional gas chromatography: a challenge in omic studies. *Trends in Analytical Chemistry*. https://doi.org/10.1016/j.trac.2018.06.005

Cordero, C., Rubiolo, P., Cobelli, L., Stani, G., Miliazza, A., Giardina, M., … Bicchi, C. (2015). Potential of the reversed-inject differential flow modulator for comprehensive two-dimensional gas chromatography in the quantitative profiling and fingerprinting of essential oils of different complexity. *Journal of Chromatography A*, *1417*, 79–95. https://doi.org/10.1016/j.chroma.2015.09.027

Cordero, C., Rubiolo, P., Reichenbach, S. E., Carretta, A., Cobelli, L., Giardina, M., & Bicchi, C. (2017). Method translation and full metadata transfer from thermal to differential flow modulated comprehensive two dimensional gas chromatography: Profiling of suspected fragrance allergens. *Journal of Chromatography A*, *1480*, 70–82. https://doi.org/10.1016/j.chroma.2016.12.011

David, F., Hoffmann, A., & Sandra, P. (1999). Finding a Needle in a Haystack: The Analysis of Pesticides in Complex Matrices by Automated On-line LC-CGC Using a New Modular System. *LC GC Europe*, *12*(9), 550–558. Retrieved from https://www.scopus.com/inward/record.uri?eid=2-s2.0-0006520622&partnerID=40&md5=848e8b7558b45da3d32d86376812f70f

Dubois, L. M., Perrault, K. A., Stefanuto, P. H., Koschinski, S., Edwards, M., McGregor, L., & Focant, J. F. (2017). Thermal desorption comprehensive two-dimensional gas chromatography coupled to variable-energy electron ionization time-of-flight mass spectrometry for monitoring subtle changes in volatile organic compound profiles of human blood. *Journal of Chromatography A*, *1501*, 117–127. https://doi.org/10.1016/j.chroma.2017.04.026

Frauendorfer, F., Schieberle, P., & Chieberle, P. E. S. (2008). Changes in Key Aroma Compounds of Criollo Cocoa Beans During Roasting Changes in Key Aroma Compounds of Criollo Cocoa Beans During Roasting, 10244–10251. https://doi.org/10.1021/jf802098f

Gharbi, I., Moret, S., Chaari, O., Issaoui, M., Conte, L. S., Lucci, P., & Hammami, M. (2017). Evaluation of hydrocarbon contaminants in olives and virgin olive oils from Tunisia. *Food Control*, *75*, 160–

166. https://doi.org/10.1016/j.foodcont.2016.12.003

Giardina, M., McCurry, J. D., Cardinael, P., Semard-Jousset, G., Cordero, C., & Bicchi, C. (2018). Development and validation of a pneumatic model for the reversed-flow differential flow modulator for comprehensive two-dimensional gas chromatography. *Journal of Chromatography A*, *1577*, 72–81. https://doi.org/10.1016/j.chroma.2018.09.022

Giddings, J. C. (1995). Sample dimensionality: A predictor of order-disorder in component peak distribution in multidimensional separation. *Journal of Chromatography A*, *703*(1–2), 3–15. https://doi.org/10.1016/0021-9673(95)00249-M

Griffith, J. F., Winniford, W. L., Sun, K., Edam, R., & Luong, J. C. (2012). A reversed-flow differential flow modulator for comprehensive two-dimensional gas chromatography. *Journal of Chromatography A*, *1226*, 116–123. https://doi.org/10.1016/j.chroma.2011.11.036

Grob, K. (2018a). Mineral oil hydrocarbons in food: a review. *Food Additives and Contaminants - Part A Chemistry, Analysis, Control, Exposure and Risk Assessment*, *35*(9), 1845–1860. https://doi.org/10.1080/19440049.2018.1488185

Grob, K. (2018b). Toxicological Assessment of Mineral Hydrocarbons in Foods: State of Present Discussions. *Journal of Agricultural and Food Chemistry*, *66*(27), 6968–6974. https://doi.org/10.1021/acs.jafc.8b02225

Grob, K., Lanfranchi, M., Egli, J., & Artho, A. (1991). Determination of food contamination by mineral oil from jute sacks using coupled LC-GC. *Journal - Association of Official Analytical Chemists*, *74*(3), 506—512. Retrieved from http://europepmc.org/abstract/MED/1874696

Haghighi, F., Talebpour, Z., & Sanati-Nezhad, A. (2015). Through the years with on-a-chip gas chromatography: A review. *Lab on a Chip*, *15*(12), 2559–2575. https://doi.org/10.1039/c5lc00283d

Jennerwein, M. K., Eschner, M., Gröger, T., Wilharm, T., & Zimmermann, R. (2014). Complete Group-Type Quantification of Petroleum Middle Distillates Based on Comprehensive Two-Dimensional Gas Chromatography Time-of-Flight Mass

Spectrometry (GC×GC-TOFMS) and Visual Basic Scripting. *Energy & Fuels*, *28*(9), 5670–5681. https://doi.org/10.1021/ef501247h

Klee, M. S., & Blumberg, L. M. (2002). Theoretical and Practical Aspects of Fast Gas Chromatography and Method Translation. *Journal of Chromatographic Science*, *40*(5), 234–247. https://doi.org/10.1093/chromsci/40.5.234

Klee, M. S., Cochran, J., Merrick, M., & Blumberg, L. M. (2015). Evaluation of conditions of comprehensive two-dimensional gas chromatography that yield a near-theoretical maximum in peak capacity gain. *Journal of Chromatography A*, *1383*, 151–159. https://doi.org/10.1016/j.chroma.2015.01.031

Krupčík, J., Gorovenko, R., Špánik, I., Sandra, P., & Giardina, M. (2016). Comparison of the performance of forward fill/flush and reverse fill/flush flow modulation in comprehensive two-dimensional gas chromatography. *Journal of Chromatography A*, *1466*, 113–128. https://doi.org/10.1016/j.chroma.2016.08.032

Kulsing, C., Nolvachai, Y., Zeng, A. X., Chin, S.-T., Mitrevski, B., & Marriott, P. J. (2014). From molecular structures of ionic liquids to predicted retention of fatty acid methyl esters in comprehensive two-dimensional gas chromatography. *ChemPlusChem*, *79*(6), 790–797. https://doi.org/10.1002/cplu.201300410

Liu, Z., & Phillips, J. B. (1994). Sensitivity and detection limit enhancement of gas chromatographic detection by thermal modulation. *Journal of Microcolumn Separations*, *6*(3), 229–235. https://doi.org/10.1002/mcs.1220060306

Magagna, F., Cordero, C., Cagliero, C., Liberto, E., Rubiolo, P., Sgorbini, B., & Bicchi, C. (2017). Black tea volatiles fingerprinting by comprehensive two-dimensional gas chromatography – Mass spectrometry combined with high concentration capacity sample preparation techniques: Toward a fully automated sensomic assessment. *Food Chemistry*, *225*, 276–287. https://doi.org/10.1016/j.foodchem.2017.01.003

Magagna, F., Liberto, E., Reichenbach, S. E., Tao, Q., Carretta, A.,

Cobelli, L., … Cordero, C. (2018). Advanced fingerprinting of high-quality cocoa: Challenges in transferring methods from thermal to differential-flow modulated comprehensive two dimensional gas chromatography. *Journal of Chromatography. A*, *1535*, 122–136. https://doi.org/10.1016/j.chroma.2017.07.014

Maikhunthod, B., Morrison, P. D., Small, D. M., & Marriott, P. J. (2010). Development of a switchable multidimensional/comprehensive two-dimensional gas chromatographic analytical system. *Journal of Chromatography A*, *1217*(9), 1522–1529. https://doi.org/10.1016/j.chroma.2009.12.078

Majors, R. E. (1980). MULTIDIMENSIONAL HIGH PERFORMANCE LIQUID CHROMATOGRAPHY. *Journal of Chromatographic Science*, *18*(10), 571–579. https://doi.org/10.1093/chromsci/18.10.571

Manzano, P., Arnáiz, E., Diego, J. C., Toribio, L., García-Viguera, C., Bernal, J. L., & Bernal, J. (2011a). Comprehensive two-dimensional gas chromatography with capillary flow modulation to separate FAME isomers. *Journal of Chromatography A*, *1218*(30), 4952–4959. https://doi.org/10.1016/j.chroma.2011.02.002

Manzano, P., Arnáiz, E., Diego, J. C., Toribio, L., García-Viguera, C., Bernal, J. L., & Bernal, J. (2011b). Comprehensive two-dimensional gas chromatography with capillary flow modulation to separate FAME isomers. *Journal of Chromatography A*, *1218*(30), 4952–4959. https://doi.org/10.1016/j.chroma.2011.02.002

Mittermüller, M., & Volmer, D. A. (2012). Micro- and nanostructures and their application in gas chromatography. *Analyst*, *137*(14), 3195–3201. https://doi.org/10.1039/c2an35184f

Moret, S., Grob, K., & Conte, L. S. (1996). On-line high-performance liquid chromatography-solvent evaporation-high-performance liquid chromatography-capillary gas chromatography-flame ionisation detection for the analysis of mineral oil polyaromatic hydrocarbons in fatty foods. *Journal of Chromatography A*,

750(1–2), 361–368. https://doi.org/10.1016/0021-9673(96)00453-0

Nicolotti, L., Cordero, C., Bressanello, D., Cagliero, C., Liberto, E., Magagna, F., … Bicchi, C. (2014). Parallel dual secondary column-dual detection: A further way of enhancing the informative potential of two-dimensional comprehensive gas chromatography. *Journal of Chromatography A*, *1360*, 264–274. https://doi.org/10.1016/j.chroma.2014.07.081

NIST/EPA/NIH Mass Spectral Library with Search Program Data Version: NIST v17. (n.d.).

Nolvachai, Y., Kulsing, C., & Marriott, P. J. (2015). Thermally sensitive behavior explanation for unusual orthogonality observed in comprehensive two-dimensional gas chromatography comprising a single ionic liquid stationary phase. *Analytical Chemistry*, *87*(1), 538–544. https://doi.org/10.1021/ac5030039

Payagala, T., Zhang, Y., Wanigasekara, E., Huang, K., Breitbach, Z. S., Sharma, P. S., … Armstrong, D. W. (2009). Trigonal Tricationic Ionic Liquids: A Generation of Gas Chromatographic Stationary Phases. *Analytical Chemistry*, *81*(1), 160–173. https://doi.org/10.1021/ac8016949

Peacock, P. M., Zhang, W.-J., & Trimpin, S. (2017). Advances in Ionization for Mass Spectrometry. *Analytical Chemistry*, *89*(1), 372–388. https://doi.org/10.1021/acs.analchem.6b04348

Perez, M., Alario, J., Vazquez, A., & Villén, J. (1999). On-line reversed phase LC-GC by using the new TOTAD (Through Oven Transfer Adsorption Desorption) interface: Application to parathion residue analysis. *Journal of Microcolumn Separations*, *11*(8), 582–589. https://doi.org/10.1002/(SICI)1520-667X(1999)11:8<582::AID-MCS3>3.0.CO;2-E

Prebihalo, S. E., Berrier, K. L., Freye, C. E., Bahaghighat, H. D., Moore, N. R., Pinkerton, D. K., & Synovec, R. E. (2017). Multidimensional Gas Chromatography: Advances in Instrumentation, Chemometrics, and Applications. *Analytical Chemistry*, acs.analchem.7b04226. https://doi.org/10.1021/acs.analchem.7b04226

Prebihalo, S. E., Berrier, K. L., Freye, C. E., Bahaghighat, H. D., Moore,

N. R., Pinkerton, D. K., & Synovec, R. E. (2018). Multidimensional Gas Chromatography: Advances in Instrumentation, Chemometrics, and Applications. *Analytical Chemistry*, *90*(1), 505–532. https://doi.org/10.1021/acs.analchem.7b04226

Purcaro, G., Moret, S., & Conte, L. (2013). Sample pre-fractionation of environmental and food samples using LC-GC multidimensional techniques. *TrAC - Trends in Analytical Chemistry*, *43*, 146–160. https://doi.org/10.1016/j.trac.2012.10.007

Reichardt, C. (2005). Polarity of ionic liquids determined empirically by means of solvatochromic pyridinium N-phenolate betaine dyes. *Green Chemistry*, *7*(5), 339–351. https://doi.org/10.1039/B500106B

Reichenbach, S. E., Carr, P. W., Stoll, D. R., & Tao, Q. (2009). Smart Templates for peak pattern matching with comprehensive two-dimensional liquid chromatography. *Journal of Chromatography A*, *1216*(16), 3458–3466. https://doi.org/10.1016/j.chroma.2008.09.058

Reichenbach, S. E., Tian, X., Cordero, C., & Tao, Q. (2012). Features for non-targeted cross-sample analysis with comprehensive two-dimensional chromatography. *Journal of Chromatography A*, *1226*, 140–148. https://doi.org/10.1016/j.chroma.2011.07.046

Rubiolo, P., Sgorbini, B., Liberto, E., Cordero, C., & Bicchi, C. (2010). Analysis of the Plant Volatile Fraction. In *The Chemistry and Biology of Volatiles* (pp. 49–93). Chichester, UK: John Wiley & Sons, Ltd. https://doi.org/10.1002/9780470669532.ch3

Ryan, D., Shellie, R., Tranchida, P., Casilli, A., Mondello, L., & Marriott, P. (2004). Analysis of roasted coffee bean volatiles by using comprehensive two-dimensional gas chromatography-time-of-flight mass spectrometry. *Journal of Chromatography A*, *1054*(1–2), 57–65. https://doi.org/10.1016/j.chroma.2004.08.057

Seeley, J. V., Schimmel, N. E., & Seeley, S. K. (2018). The multi-mode modulator: A versatile fluidic device for two-dimensional gas chromatography. *Journal of Chromatography A*, *1536*, 6–15.

https://doi.org/10.1016/J.CHROMA.2017.06.030

Sgorbini, B., Cagliero, C., Acquadro, S., Marengo, A., Cordero, C., Liberto, E., … Rubiolo, P. (2019). Evaluation of volatile bioactive secondary metabolites transfer from medicinal and aromatic plants to herbal teas: Comparison of different methods for the determination of transfer rate and human intake. *Journal of Chromatography A*. https://doi.org/https://doi.org/10.1016/j.chroma.2019.02.012

Sgorbini, B., Cagliero, C., Boggia, L., Liberto, E., Reichenbach, S. E., Rubiolo, P., … Bicchi, C. (2015). Parallel dual secondary-column-dual detection comprehensive two-dimensional gas chromatography: A flexible and reliable analytical tool for essential oils quantitative profiling. *Flavour and Fragrance Journal*, *30*(5), 366–380. https://doi.org/10.1002/ffj.3255

Sharif, K. M., Kulsing, C., Junior, A. I. D. S., & Marriott, P. J. (2017). Second dimension column ensemble pressure tuning in comprehensive two-dimensional gas chromatography. *Journal of Chromatography A*. https://doi.org/10.1016/j.chroma.2017.10.060

Sharif, K. M., Kulsing, C., & Marriott, P. J. (2016). Pressure Tuning of First Dimension Columns in Comprehensive Two-Dimensional Gas Chromatography. *Analytical Chemistry*, *88*(18), 9087–9094. https://doi.org/10.1021/acs.analchem.6b02017

Smith, P. A. (2012). Person-portable gas chromatography: Rapid temperature program operation through resistive heating of columns with inherently low thermal mass properties. *Journal of Chromatography A*, *1261*, 37–45. https://doi.org/10.1016/j.chroma.2012.06.051

Terry, S. C., Herman, J. H., & Angell, J. B. (1979). A Gas Chromatographic Air Analyzer Fabricated on a Silicon Wafer. *IEEE Transactions on Electron Devices*, *26*(12), 1880–1886. https://doi.org/10.1109/T-ED.1979.19791

Tranchida, P. Q., Casilli, A., Dugo, P., Dugo, G., & Mondello, L. (2007). Generation of improved gas linear velocities in a comprehensive two-dimensional gas chromatography system. *Analytical Chemistry*, *79*(6), 2266–2275.

https://doi.org/10.1021/ac0618066

Tranchida, P. Q., Franchina, F. A., Dugo, P., & Mondello, L. (2012). A flow-modulated comprehensive gas chromatography-mass spectrometry method for the analysis of fatty acid profiles in marine and biological samples. *Journal of Chromatography A*, *1255*, 171–176. https://doi.org/10.1016/j.chroma.2012.02.016

Tranchida, P. Q., Purcaro, G., Dugo, P., Mondello, L., & Purcaro, G. (2011). Modulators for comprehensive two-dimensional gas chromatography. *TrAC - Trends in Analytical Chemistry*, *30*(9), 1437–1461. https://doi.org/10.1016/j.trac.2011.06.010

van Den Dool, H., & Dec. Kratz, P. (1963). A generalization of the retention index system including linear temperature programmed gas—liquid partition chromatography. *Journal of Chromatography A*, *11*, 463–471. https://doi.org/10.1016/S0021-9673(01)80947-X

Vreuls, J. J., de Jong, G. J., & Brinkman, U. A. T. (1991). On-line coupling of liquid chromatography, capillary gas chromatography and mass spectrometry for the determination and identification of polycyclic aromatic hydrocarbons in vegetable oils. *Chromatographia*, *31*(3–4), 113–118. https://doi.org/10.1007/BF02274556

Weber, S., Schrag, K., Mildau, G., Kuballa, T., Walch, S. G., & Lachenmeier, D. W. (2018). Analytical Methods for the Determination of Mineral Oil Saturated Hydrocarbons (MOSH) and Mineral Oil Aromatic Hydrocarbons (MOAH)—A Short Review. *Analytical Chemistry Insights*, *13*, 1177390118777757. https://doi.org/10.1177/1177390118777757

Wong, Y. F., Perlmutter, P., & Marriott, P. J. (2017). Untargeted metabolic profiling of Eucalyptus spp. leaf oils using comprehensive two-dimensional gas chromatography with high resolution mass spectrometry: Expanding the metabolic coverage. *Metabolomics*, *13*(5), 1–17. https://doi.org/10.1007/s11306-017-1173-3

Yan, D. D., Wong, Y. F., Tedone, L., Shellie, R. A., Marriott, P. J., Whittock, S. P., & Koutoulis, A. (2017). Chemotyping of new hop (Humulus lupulus L.) genotypes using comprehensive two-

dimensional gas chromatography with quadrupole accurate mass time-of-flight mass spectrometry. *Journal of Chromatography* *A*. https://doi.org/10.1016/j.chroma.2017.08.020

Figure captions

Figure 9.1: Planar column compared to a one Euro cent coin. From Cagliero et al. (Cagliero et al., 2016).

Figure 9.2: GC profiles (**9.2A**) of chamomile e.o. obtained with the FFAP–EXT planar column 2 (solid line), compared to the reference (ref. 2) NB column (dashed line), and (**9.2B**) of chamomile headspace sampled by SPME. Analysis conditions: temperature program: 50 °C//15 °C/min//190 °C, flow rate: EOF (see Table 9.1). Peak identification: 1: farnesene, 2: germacrene D, 3: bisabolol oxide B, 4: bisabolone oxide B, 5: α-bisabolol, 6: chamazulene, 7: bisabolol oxide A, 8: spiroether. From Cagliero et al. (Cagliero et al., 2016).

Figure 9.3: GC profiles of sage e.o. obtained with (**9.3A**) the Sil-5%-PH planar column 1 and (**9.3B**) with the reference Sil-5%-PH NB column (Ref. 1). Analysis conditions: temperature program: 50 °C//5 °C/min//190 °C for (**9.3A**) and 50 °C//2.2 °C/min//190 °C (translated method) for (**9.3B**), flow rate: EOF (see Table 1). Peak identification: 1: α-pinene, 2: camphene, 3: β-pinene, 4: β-mircene, 5: p-cymene, 6: 1,8-cineole, 7: limonene, 8: trans β-ocimene, 9: γ-terpinene, 10: α-thujione, 11: β-thujione, 12: camphor, 13: borneol 14: bornyl acetate,15: β-caryophillene, 16: α-humulene, 17: ledene,18: caryophillene oxide, 19: sclareol. From Cagliero et al. (Cagliero et al., 2016).

Figure 9.4: Total ion chromatograms of splitless injections of roasted coffee volatiles extracted by HSSPME and analysed by using the cryofocusing technique. Furfuryl alcohol was the major peak (*) and caffeine was the last eluted peak (▼) for all evaluated columns. The HS-SPME extractions were carried out using 1.6 g of the powder sample and a PDMS/CAR/DVB (50/30 μm) fibre (Supelco, ref. 57,328-U), using in a 40-mL glass vial sealed with a plastic cap and silicone septum. The extraction method had an equilibration time of 20 min and an extraction time of 40 min at 60 °C. SPME thermal desorption was by splitless mode at 250 °C for 1 min. A SPME liner with an internal diameter of 0.75 mm (Supelco) was used. The oven temperature programme: 50 °C (1 min), 50–240°C at 3 C/min, 240 C (5 min). From Amaral et al. (Amaral et al., 2018).

Figure 9.5: Multiple Head Space-SPME-GC–MS (**9.5A**), Direct Immersion-SPME-GC–MS and DAI-GC-FID chromatographic profiles of peppermint plant material (**9.5A**) and related herbal teas (**9.5B** and **9.5C**) prepared with commercially available teabags. Peak identification: 1) limonene, 2) 1,8-cineole, 3) γ-terpinene, 4) menthone, 5) isomenthone, 6) menthol, 7) isomenthol, 8) pulegone, 9) piperitone, 10) menthyl acetate, 11) β-bourbonene, 12) trans-β-caryophyllene, 13) germacrene D. From Sgorbini et al. (Sgorbini et al., 2019).

Figure 9.6: MOSH and MOAH chromatograms from a fresh fiber box for biscuits printed with a mineral oil containing ink (left) and a fresh fiber paper tea bag with mineral ink oil and an oil probably used for paper making. CyCy, cyclohexyl cyclohexane; DIPN, diisopropyl naphthalene; MOAH, mineral oil aromatic hydrocarbon; MOSH, mineral oil saturated hydrocarbon. From Biedermann and Grob (M Biedermann et al., 2013)

Figure 9.7: Separation and orthogonality (%O) by informational theory for Tea Tree Oil oil using SLB-IL60 + SLB-5 ms 1D coupled column ensembles at (A) 65–30 psi and (B) 65–60 psi and SLB-5 ms + SLB-IL60 1D coupled column at (C) 65–30 psi and (D) 65–60 psi, Pi and Pj, respectively. From Sharif et al. (Khan M. Sharif et al., 2016)

Figure 9.8: Cod liver oil 20:80 (FID) GC × GC analysis carried out by using a 1.3 °C/min temperature program rate and an 8 s modulation period. Peak identification from the original paper: 2. C16:1ω7; 3. C16:2ω4. 4. C16:4ω3. Split flow GC × GC analyses were carried out on: Equity-5MS 30 m × 0.25 mm i.d., 0.25 μm d_f column was serially connected by using a Y press fit (Mega, Legnano, Italy) to a Supelcowax 10 1 m × 0.1 mm i.d., 0.1 μm d_f column. The latter was passed through the thermal modulator (LMCS) and connected to the FID. A 0.3 m × 0.1 mm i.d. retention gap (Mega) was also connected to a Y press fit and then to a manual-type needle valve located on top of the GC oven. The analysis was carried out

with a 20:80 (FID) split flow GC × GC, injection volume, 4.0 µL, in split mode (4:1 ratio); hydrogen inlet pressure, 166.3 kPa. From Tranchida et al. (Peter Quinto Tranchida et al., 2007)

Figure 9.9: 2D plots of *Artemisia umbelliformis* essential oil; the magnified region corresponds to the elution area of 2-methylbutyl isovalerate, nonanal and α-thujone. **9.9A**: separation pattern obtained from a ^{1}D 30 m, 0.25 mm d_c, 0.25 µm d_f SE52 (95% polydimethylsiloxane, 5% phenyl) Mega (Legnano, Milan, Italy) coupled to two-parallel ^{2}D 1.4 m, 0.1 mm d_c, 0.10 µm d_f OV1701 (86% polydimethylsiloxane, 7% phenyl, 7% cyanopropyl) plus a deactivated capillary to MS detector of 0.17 m, 0.1 mm d_c Mega (Legnano, Milan, Italy); **9.9B** separation pattern obtained from a conventional set-up with 2D post-column splitting to MS/FID (50:50) with a ^{1}D 30 m, 0.25 mm d_c, 0.25 µm d_f SE52 (95% polydimethylsiloxane, 5% phenyl) Mega (Legnano, Milan, Italy) coupled to a single ^{2}D 1.4 m, 0.1 mm d_c, 0.10 µm d_f OV1701 (86% polydimethylsiloxane, 7% phenyl, 7% cyanopropyl) and deactivated capillaries for effluent splitting to parallel detectors 0.4 m, 0.1 mm d_c to MS and 0.25 m, 0.1 mm d_c to FID all capillaries were from Mega (Legnano, Milan, Italy). For pressure settings refer to the original paper. Adapted from Nicolotti et al. (Nicolotti et al., 2014).

Figure 9.10: Pseudocolorized GC×GC chromatogram of volatiles sampled by HS-SPME on dry leaves and water addition of a black tea sample from (**9.10A**). Volatiles were sampled by HS-SPME and analyzed on a system configured as follows: ^{1}D SE52 column (95% polydimethylsiloxane, 5% phenyl) (30 m × 0.25 mm d_c, 0.25 µm d_f) coupled with a ^{2}D OV1701 column (86% polydimethylsiloxane, 7% phenyl, 7% cyanopropyl) (1 m × 0.1 mm d_c, 0.10 µm d_f). Columns were from Mega (Legnano, Milan, Italy). Carrier gas was helium, kept at a constant flow with an initial head pressure 298 kPa. The temperature program was 50°C (1 min) to 280°C (10 min) at 2.5°C/min. For further detail see the original paper from Magagna et al. (Magagna et al., 2017). Pink-colored circles highlight 2D peaks where the scripting function: [Relative(43)>0.98)&(Relative(57)>0.78)&(Relative(71)>0.68)&(Relative(85)>0.50] was verified - normal and iso-alkanes (**9.10B**). Green and cyano colored circles highlight 2D peaks where the scripting function:
[AND((Relative(41)>0.70)&(Relative(44)>0.70)&(Relative(57)>0.50)),((Relative(41)>0.90)&(Relative(55)>0.70)&(Relative(69)>0.40)&(Relative(83)>0.40))] was verified - saturated and unsaturated-aldehydes (**9.10C**).

Figure 9.11: Schematic diagram of the switchable targeted MDGC/GC GC × GC system. DS: Deans switch; CT: cryotrap; ^{1}D: first dimension column; ^{2}D$_S$: short second dimension column (for GC × GC mode) terminated at Flame Ionization detector FID 1; ^{2}D$_L$: long second dimension column (for targeted MDGC mode) terminated at Flame Ionization detector FID 2. From Maikhunthod et al. (Maikhunthod et al., 2010).

Figure 9.12: Schematic diagram of the Agilent Technologies reverse-inject differential flow modulator in loading state (**9.12A**) and injection state (**9.12B**). From Cordero et al. (Cordero et al., 2015).

Figure 9.13: 2D pattern of a roasted Chontalpa cocoa sample analyzed with a reference method developed on the loop-type TM platform (**9.13A**) and with the translated method by reverse-inject FM platform (**9.13B**). Pink circles indicate the positions of targeted peaks. (**9.13C**) Illustrates the translated method 2D pattern with the over-imposed untargeted template (green circles indicate *realiable* peaks while red graphics delineate *peak-regions*). (**9.13D**) shows the 2D pattern from the non translated FM GC × GC–MS method (for chromatographic conditions see the refrence paper (Magagna et al., 2018)).

Figure 9.14: Spectral profiles for nonanal (**9.14A**) and limonene (**9.14B**) at 70 eV, 12 eV and 14 eV. Spectral comparisons are between 12 eV and 14 eV (**9.14A-I** and **9.14B-I**; between 12 eV and 70 eV (**9.14A-II** and **9.14B-II**) and between 14 eV and 70 eV (**9.14A-III** and **9.14B-III**). Green text below spectra refers DMF and RMF values. From reference (Baroux et al., 2018).

Table captions

Table 9.1: planar and conventional column characteristics and chromatographic conditions.

Table 9.2: Highly thermally stable ionic liquids with multi charges used as stationary phase in gas chromatography. Modified from (Berthod et al., 2018).

Table 9.3 Direct and Reverse Match Factor (DMF and RMF) values for a series of targeted analytes representing different functionalities. Data refers of spectral similarity between 70 eV vs. database (Wiley 7n or NIST 2014); b) 12 eV vs. 14 eV; c) 12 eV vs. 70 eV; d) 14 eV vs. 70 eV. Signal-to-noise ratio (SNR) values are those corresponding to peak-apex and recorded at 12 and 70 eV. Their ratio (12 eV / 70 eV) is also reported to facilitate comparisons. From (Baroux et al., 2018).

Figures

Figure 9.1
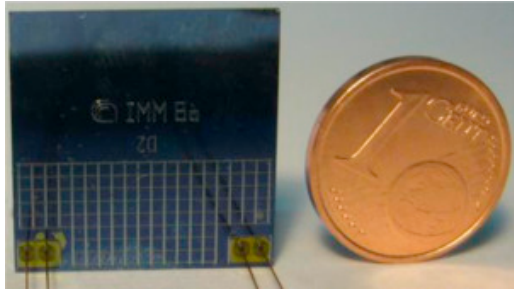
Figure 9.2
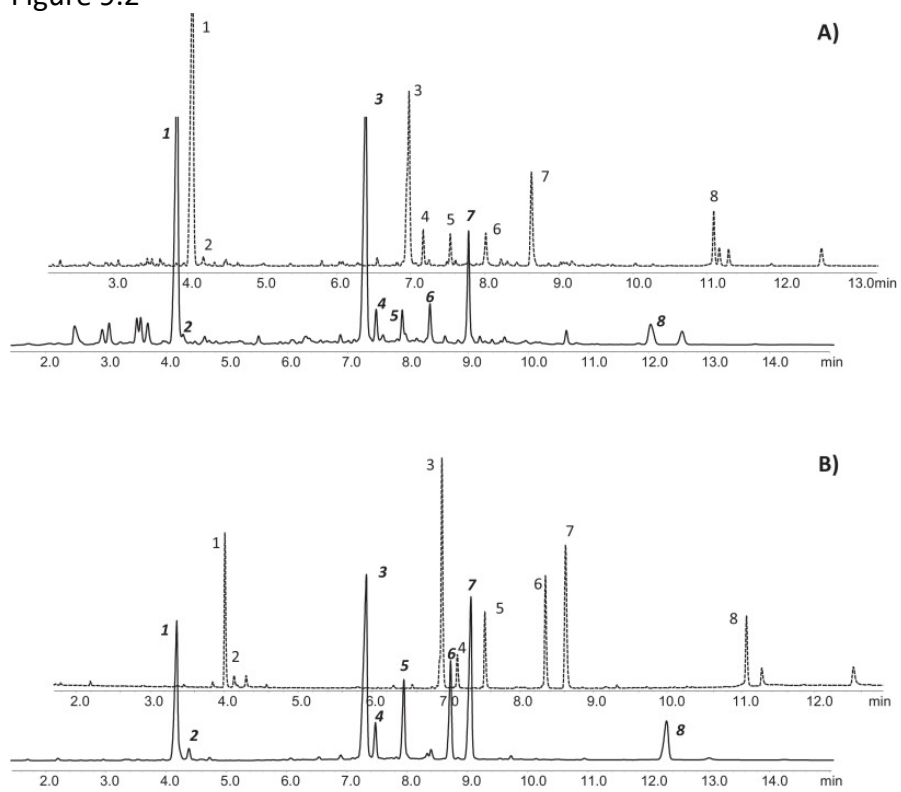
Figure 9.3

Figure 9.4

Figure 9.5

MHS-SPME-GC-MS raw peppermint A

DI-SPME-GC-MS peppermint herbal tea B

DAI-GC-FID peppermint herbal tea C
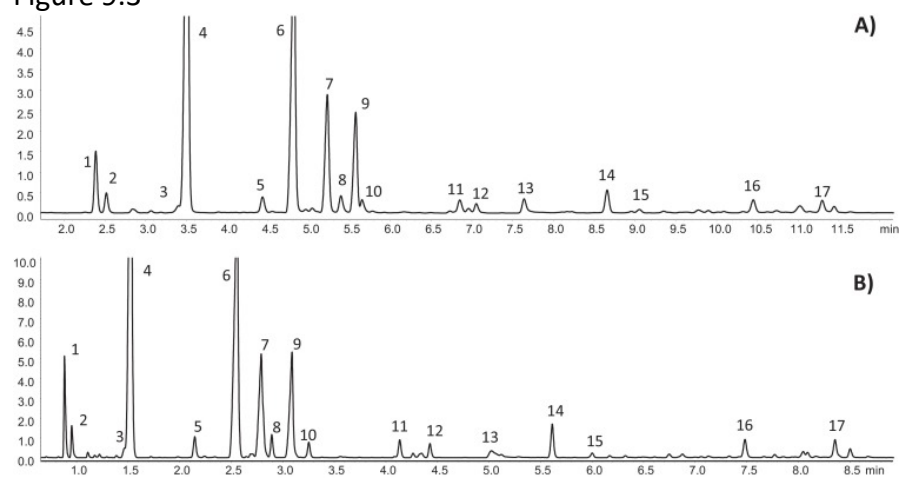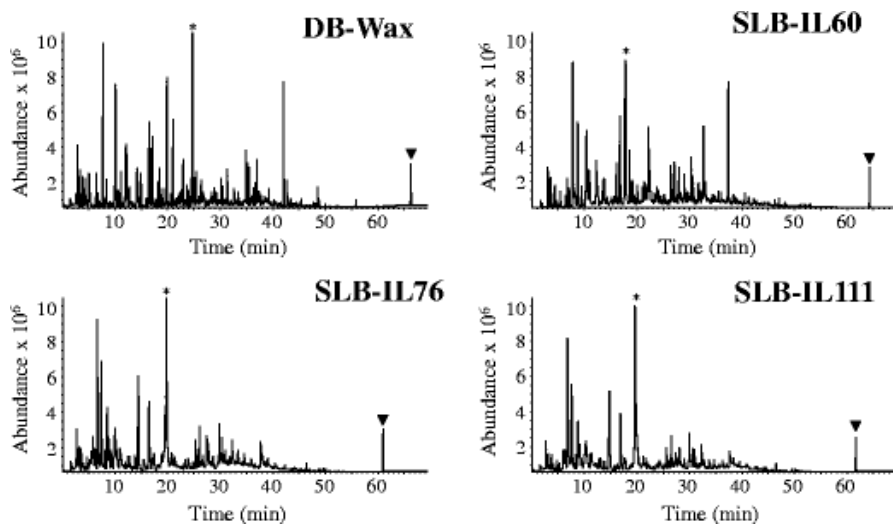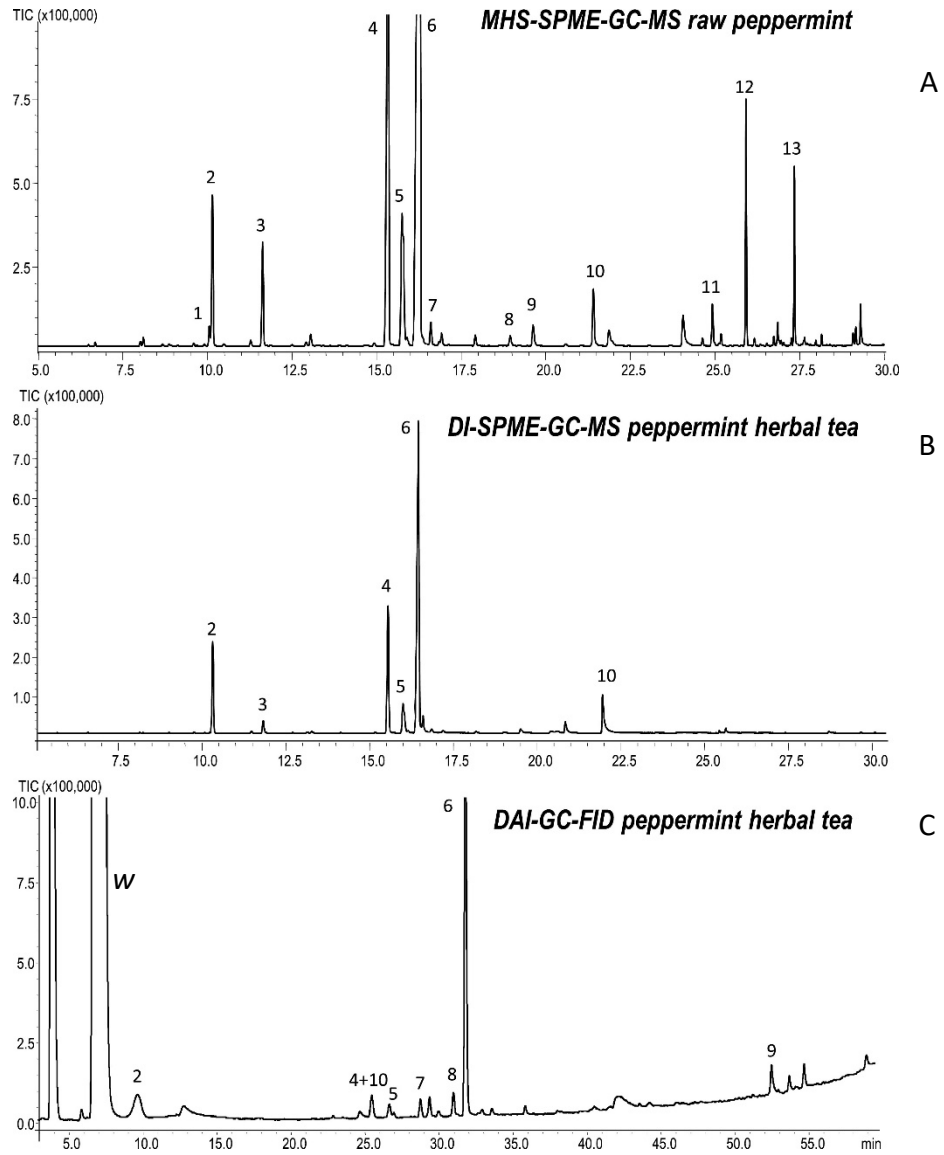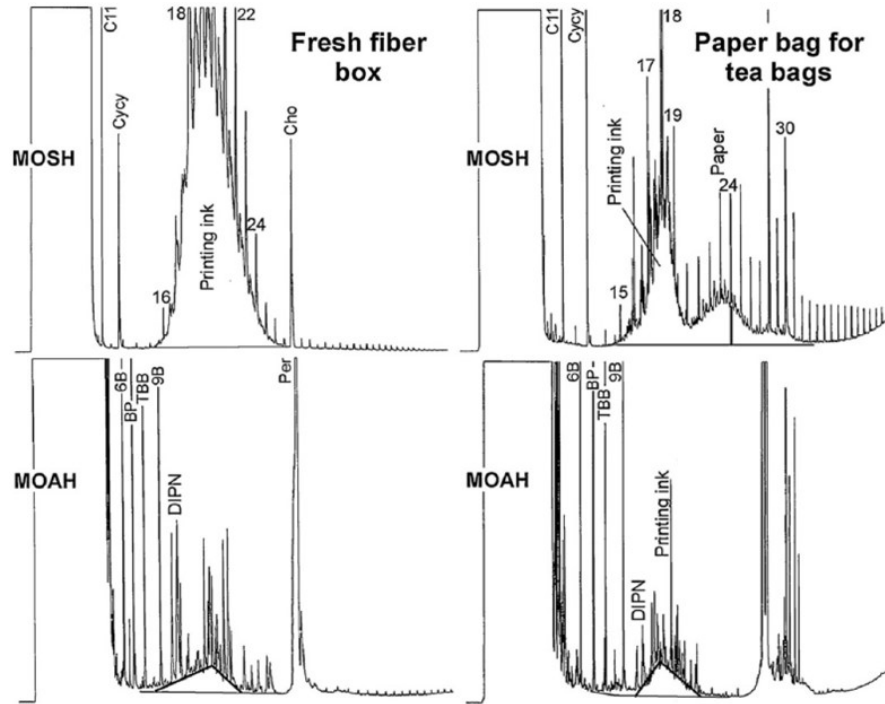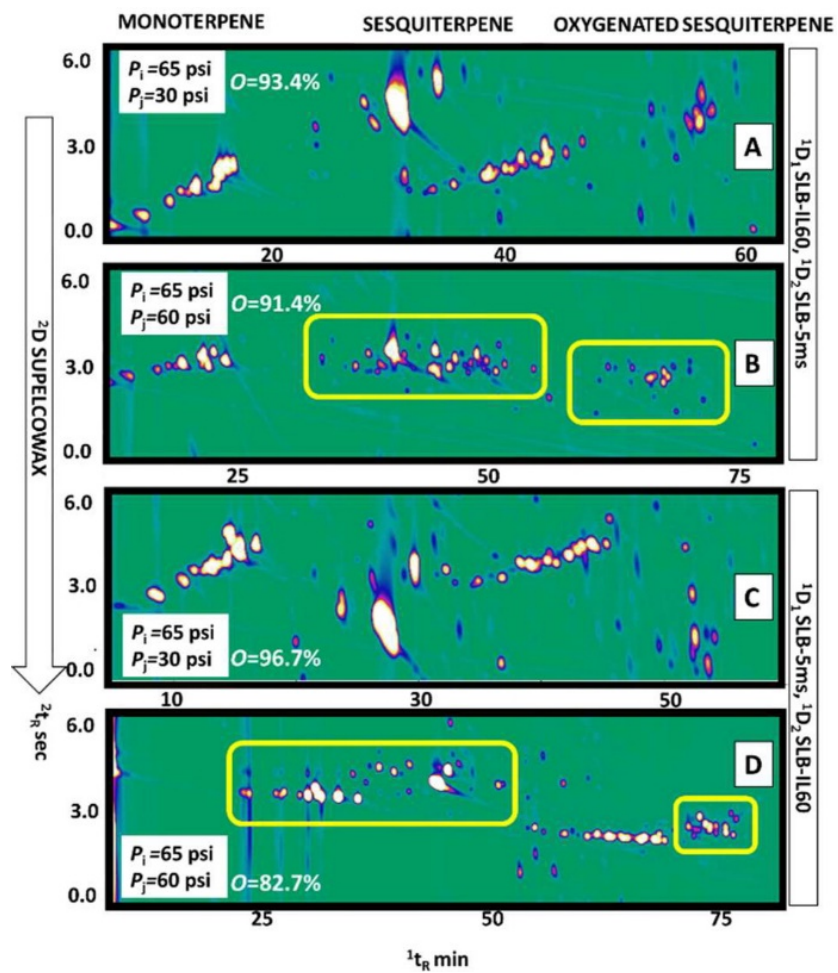
Figure 9.6

Figure 9.7

Figure 9.8
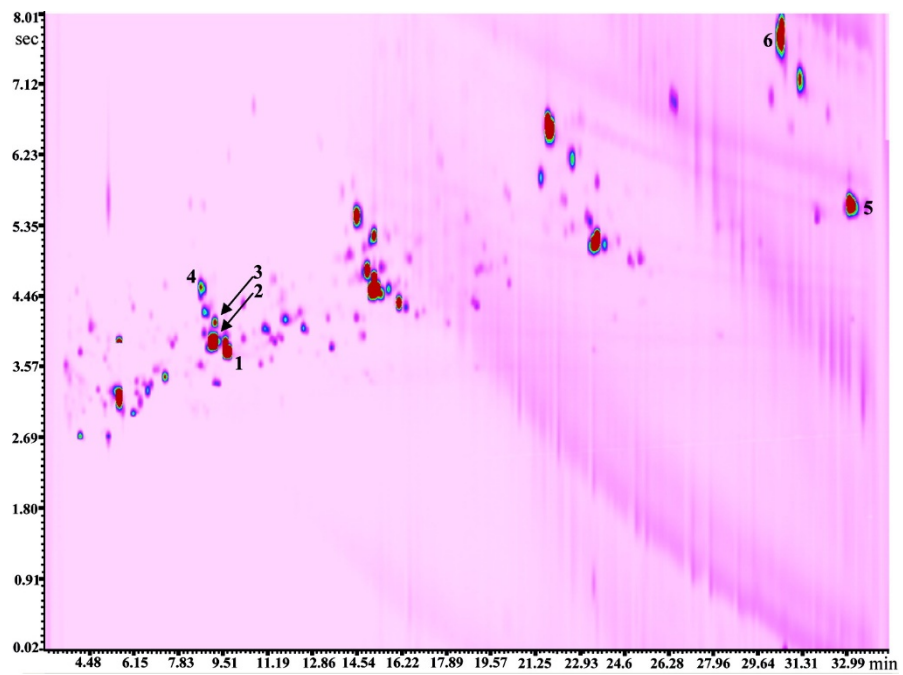
Figure 9.9
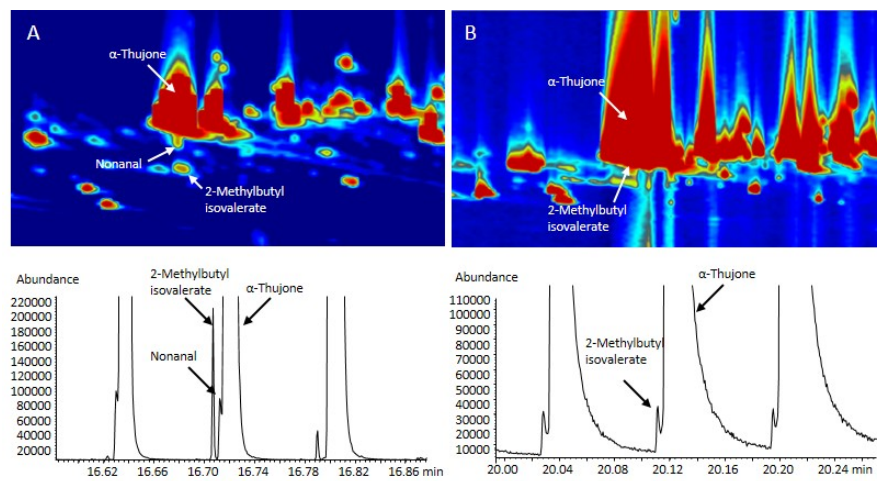
Figure 9.10
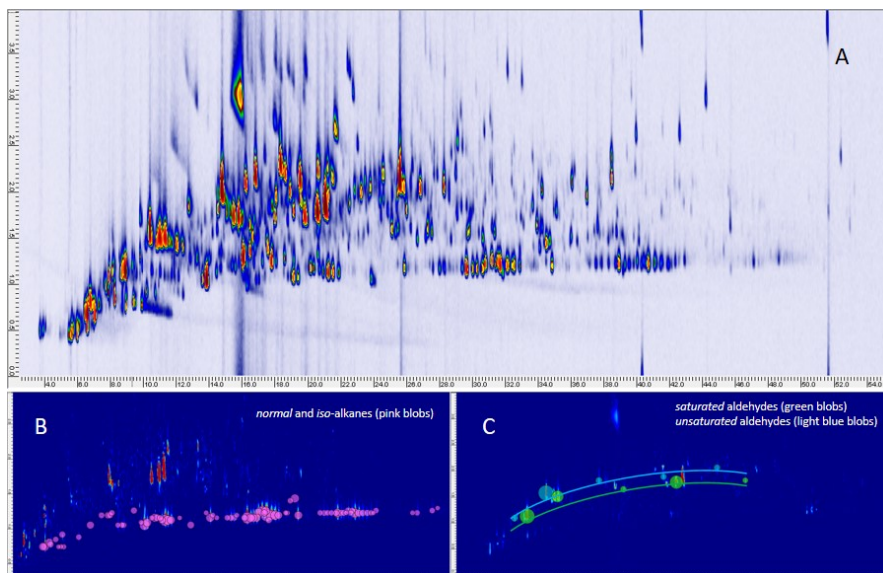
Figure 9.11
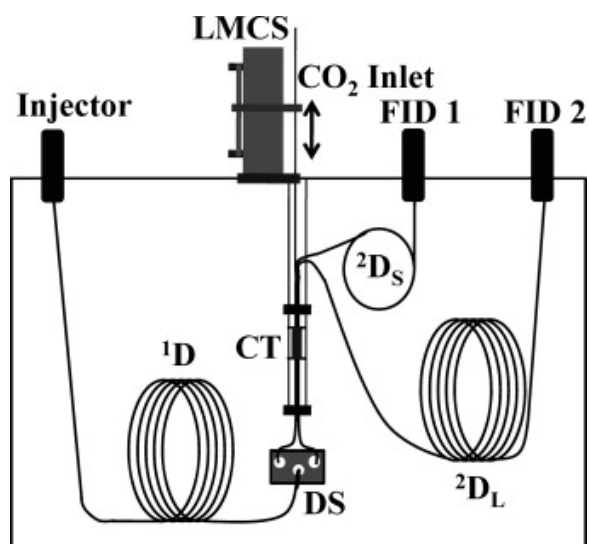
Figure 9.12

A-loading
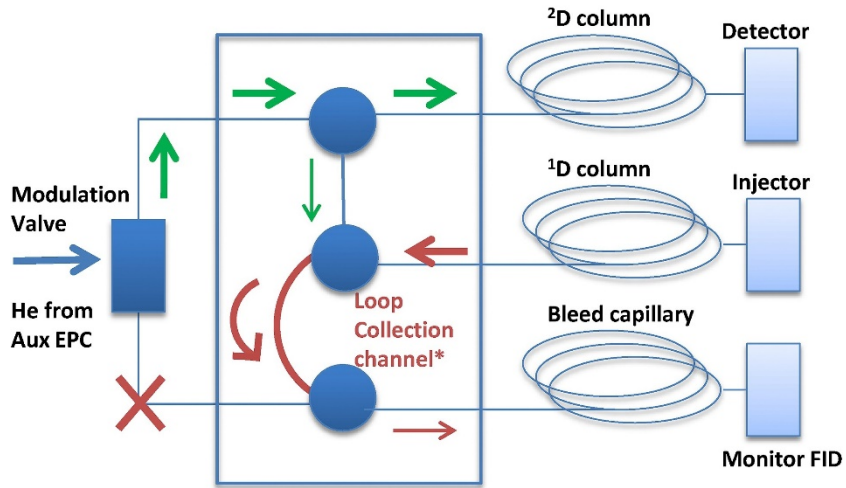
B-inject
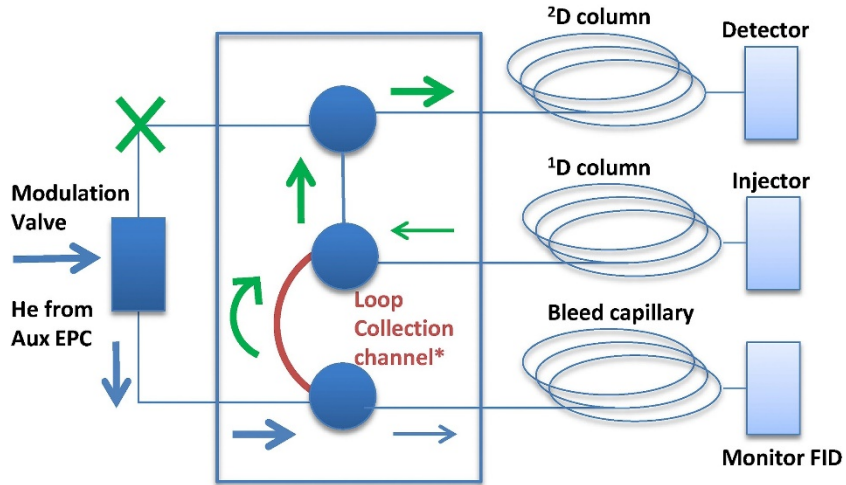
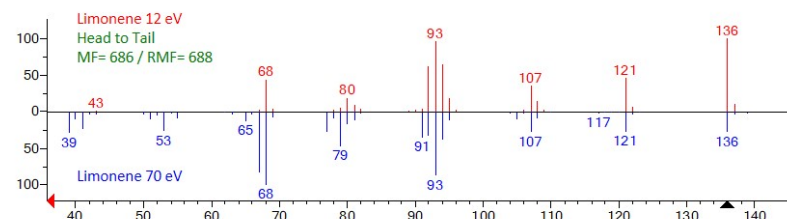
* Rough representation of internal channel

Figure 9.13
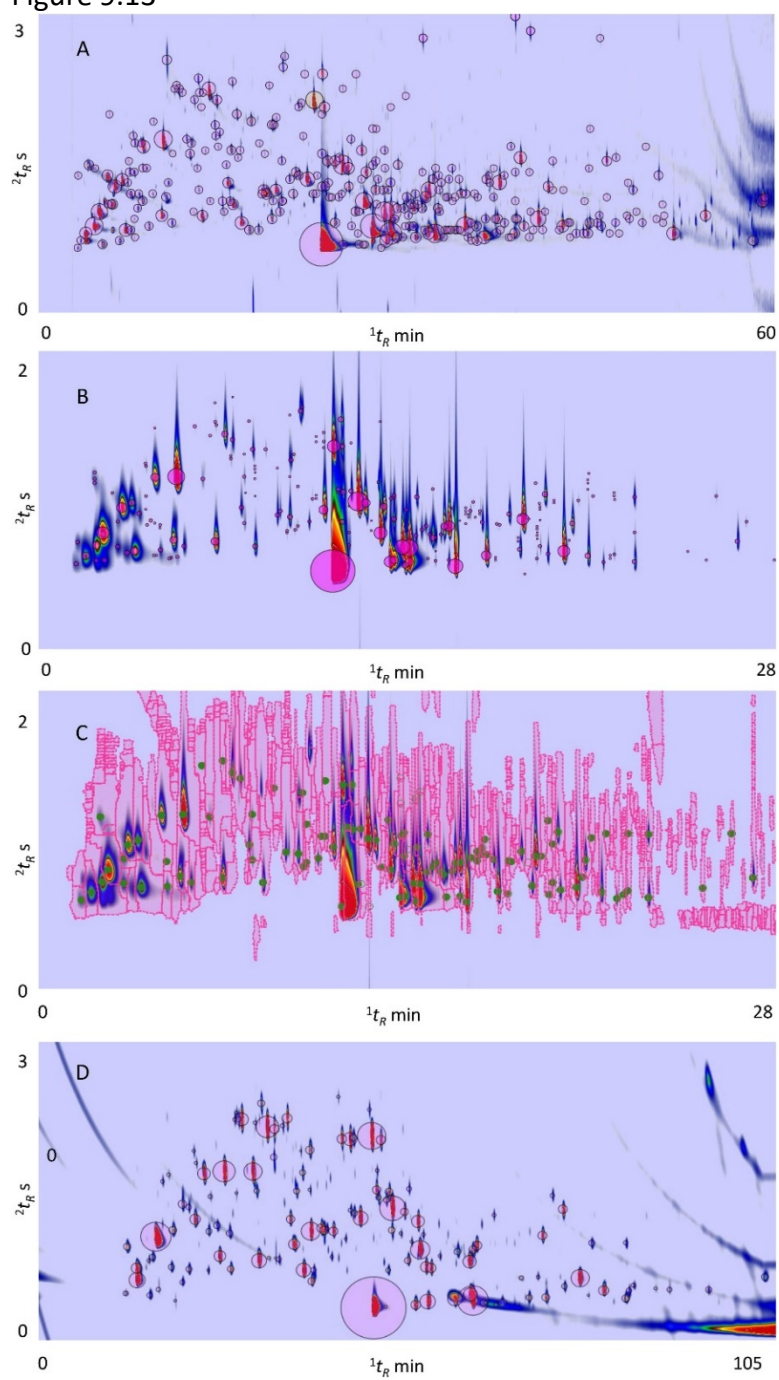
Figure 9.14
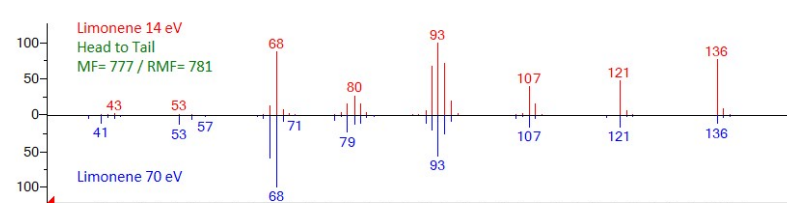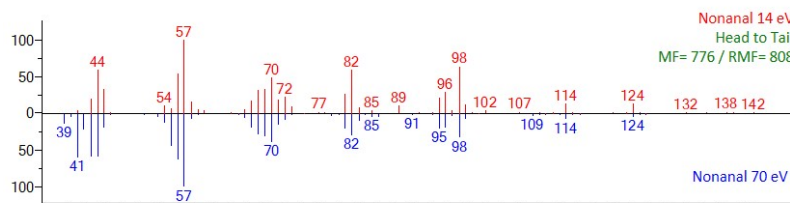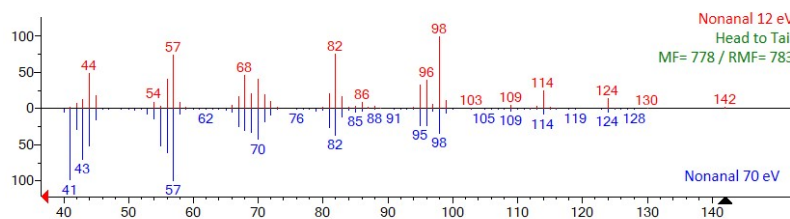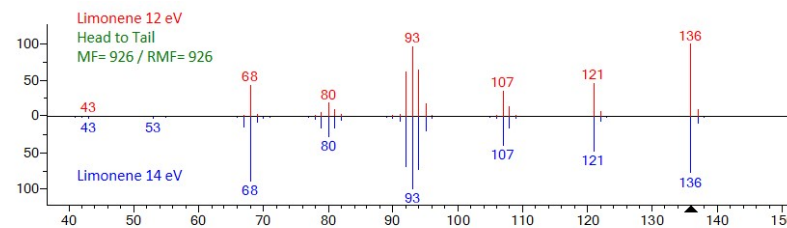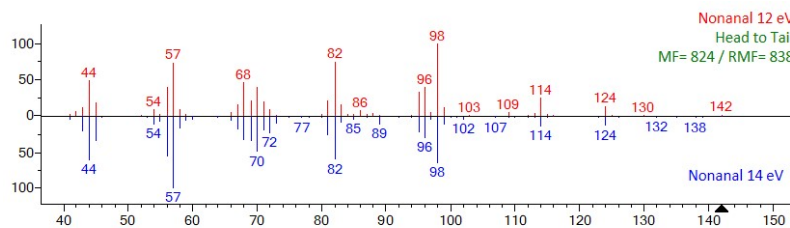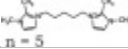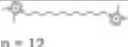
Tables

Table 9.1

Column #	Phase	Length (cm)	Width (µm)	Depth (µm)	Nom. d_c (µm)	Nom. d_f (µm)	Coating. SP conc. (mg/10mL)	N	N/m	S	EOF mL/min	Linear vel. cm/s	Pressure Kpa
1	Sil-5%-PH	200	50	50	56	0.28	200	13512	6756	463	0.4	114.7	203
Ref. 1	Sil-5%-PH	5 m	circ 100		100	0.10	40	37151	7430	641	0.4	59.9	90.8
2	FFAP–EXT	168	50	80	71	0.10	56	10263	6109	270	0.4	104.1	111.5
3	FFAP–EXT	168	50	80	71	0.22	120	12209	7267	419	0.4	104.1	112.5
Ref. 2	FFAP–EXT	5 m	circ 100		100	0.10	40	37516	7503	598	0.4	59.9	90.8

Table 9.2

Name[a]	Structure	m.w.	m.p. °C	Rochschneider McReynolds polarity	Decomp. temp. °C	Trade name	Max working temp. °C
Dicationic bis(trifluoromethylsulfonyl)imide							
n = 10	C32H62F12N2O8P2S4	1020	50		425		
n = 10							
n = 12	C34H66F12N2O8P2S4	1048	25	2760	425	**SLB-IL60**	300
3 PEG unit	C30H58F12N2O11P2S4	1040	26		410		
3 PEG unit							
n = 12	C24H30F12N6O8S4	806	−26		350		
n = 12							
n = 5	19H26F12N6O8S4	822		4938	390	**SLB-IL111**	270
n = 5							
n = 12	C26H45F12N6O8S4	925	−20	3741	390	**SLB-IL82**	270
n = 12							
n = 9	C23H30F12N6O8S4	874	−15	4357	350	**SLB-IL100**	230
n = 9							
Tricationic bis(trifluoromethylsulfonyl)imide							
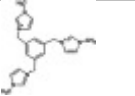
	C57H105F18N7O15P3S6	1758	−31	3509	390	**SLB-IL76**	270
	C27H27F18N9O12S6	1203	−38		414		

ⁿ is the alkyl chain length of the linkage of the two phosphonium or imidazolium cationic groups. SLB-ILxxx is the trade name of Millipore Sigma line of products along with the manufacturer recommended maximum working temperature. The xxx value is related to the Rohrschneider-McReynolds polarity constants of the IL stationary phase.

Table 9.3

Compound name	^1t_R min	^2t_R sec	I^T_S	70 eV vs. lib		12 vs.14 eV		12 vs. 70 eV		14 vs.70 eV		SNR		Ratio
				DMF	RMF	DMF	RMF	DMF	RMF	DMF	RMF	70 eV	12 eV	(12/70)
3-Methyl-butanal	8.40	1.32	911	963	963	827	833	696	694	798	805	2309	4300	**1.86**
2-Methyl-butanal	8.40	1.34	911	970	981	883	902	878	909	839	868	3791	5920	**1.56**
2,3-Pentanedione	12.40	1.24	1050	973	995	914	914	810	810	817	822	512	280	0.55
Hexanal	13.33	1.82	1077	992	993	881	880	786	789	868	872	237	69	0.29
β-Pinene	14.27	3.20	1104	974	979	918	924	693	694	796	796	43	31	0.72
3-Penten-2-one	15.20	1.52	1128	983	989	850	850	682	684	835	836	765	384	0.50
Limonene	17.80	1.04	1197	985	986	926	926	717	724	773	786	277	150	0.54
Hexyl acetate	21.07	0.92	1280	982	985	922	928	737	745	911	912	529	142	0.27
Octanal	21.60	0.80	1293	990	990	848	853	805	840	793	820	50	18	0.36
Nonanal	25.60	1.16	1397	974	989	824	838	778	783	776	808	658	455	0.69
Furfural	27.93	1.78	1459	985	990	876	877	803	805	863	883	529	590	**1.12**
Benzaldehyde	30.60	0.58	1533	974	984	964	964	837	837	717	723	2296	2640	**1.15**
2(E)-Nonenal	30.80	1.74	1538	975	976	922	931	805	840	832	837	419	197	0.47
Linalool	31.20	1.36	1550	978	988	919	923	771	776	851	853	605	394	0.65
1-Octanol	31.67	0.62	1563	996	996	887	889	815	829	864	889	294	105	0.36
2-Furan methanol	34.60	1.30	1648	984	989	897	897	735	735	813	813	1350	2100	**1.56**
Benzyl alcohol	41.53	1.26	1862	994	995	901	901	783	787	789	789	713	450	0.63
γ-octalactone	43.33	3.04	1920	990	992	941	945	857	857	890	890	29	16	0.55
1H-Pyrrole-2-carboxaldehyde	46.13	0.84	2017	860	869	924	930	780	780	924	927	120	113	0.94
γ-Nonalactone	46.40	0.90	2026	877	978	939	949	817	817	857	862	204	95	0.47